This is to certify that the

dissertation entitled

DEGRADATION OF 3-PHENYLPROPIONIC ACID BY *HALOFERAX* SP.D1227

presented by

Weijie Fu

has been accepted towards fulfillment
of the requirements for
Ph.D. degree in Microbiology

Major professor

Date December 16, 1997

DEGRADATION OF 3-PHENYLPROPIONIC ACID BY *HALOFERAX* SP. D1227

By

Weijie Fu

A DISSERTATION

Submitted to
Michigan State University
in partial fulfillment of the requirements
for the degree of

DOCTOR OF PHILOSOPHY

Department of Microbiology

1997

ABSTRACT

DEGRADATION OF 3-PHENYLPROPIONIC ACID BY *HALOFERAX* SP. D1227

By

Weijie Fu

Haloferax sp. D1227, an extreme halophile isolated by Emerson et al. from soil contaminated with highly saline oil brine, is the only reported aerobic archaeon capable of metabolizing aromatic compounds as the sole carbon source for growth. In contrast to the extensive research on aromatic degradation by bacteria and fungi, little is known about the aromatic metabolism in Archaea, which represents a third domain of life phylogenetically distinct from Bacteria and Eucarya. The degradation of the important plant-derived aromatic compound 3-phenylpropionic acid by *Hf.* D1227 was studied to understand the archaeal strategies for phenylpropanoid catabolism. I propose that *Hf.* D1227 metabolizes 3-phenylpropionic acid by initial 2-carbon shortening of the side chain to benzoylCoA, via a mechanism similar to fatty acid β-oxidation, followed by aromatic degradation using a gentisate pathway based on the following findings: (1) the extracellular accumulation of cinnamic acid, benzoic acid,

3-hydroxybenzoic acid, and gentisic acid in the cultures of *Hf.* D1227 grown on 3-phenylpropionic acid; (2) the presence of a 3-phenylpropionyl CoA dehydrogenase; (3) the ATP-, CoA- and NAD-dependent conversion of cinnamic acid to benzoylCoA; and (4) the presence of gentisate 1,2-dioxygenase. I also demonstrated that the upper aliphatic pathway from 3-phenylpropionic acid to benzoic acid is separately regulated from the lower gentisate pathway.

The gentisate 1,2-dioxygenase involved in the 3-phenylpropionic acid degradation by *Hf.* D1227 was purified using phenyl-Sepharose CL-4B chromatography, hydroxyapatite chromatography, and gel filtration with Superose 12. The enzyme was a 174,000±6,000 Da homotetramer composed of 42,000±1,000 Da subunits. The maximal enzyme activity was obtained in 2 M KCl or NaCl, 45°C and pH 7.2. The enzyme had a 9.2% excess acidic over basic amino acids. The gene encoding *Hf.* D1227 gentisate 1,2-dioxygenase was cloned, sequenced and expressed in *H. volcanii*. Four histidine clusters (H-X-H) and a segment containing key conserved residues in eubacterial extradiol dioxygenases fingerprint region were identified in the deduced amino acid sequence of *Hf.* D1227 gentisate 1,2-dioxygenase.

To my parents and my husband for their love and support.

ACKNOWLEDGMENTS

I would like to express my sincere thanks to: Dr. Patrick Oriel, my mentor, for his guidance, kindness and patience. Dr. Michael Bagdasarian, Dr. John Breznak, Dr. Shelagh Ferguson-Miller and Dr. Robert Hausinger, my committee members, for their invaluable advice and time. Dr. Olga Maltseva and Dr. Tae-Kyou Cheong for all the helpful discussions and for teaching me many techniques. Dr. Sadhana Chauhan and Dr. Trevor D'Souza for their help at the beginning of my Ph.D. career.

PREFACE

This dissertation includes four chapters and an appendix. The first chapter is a general introduction and the fourth chapter is a summary and recommendations for future research. The second and third chapters present the results of the dissertation research in manuscript form. Both have been submitted to Extremophiles. I also participated in a project to isolate a pinene-degrading thermophile, *Bacillus pallidus* BR425. The paper presenting the results of the pinene work is included in this thesis as an appendix.

TABLE OF CONTENTS

LIST OF TABLES

LIST OF FIGURES

Chapter 1

INTRODUCTION

Objective of this study

An extremely halophilic, aerobic archaeon *Haloferax* sp. D1227 was isolated by Emerson et al. from soil contaminated with highly saline oil brine near Grand Rapids, Michigan (20). This strain requires 2 M NaCl for optimal growth and is the only reported aerobic archaeon capable of utilizing aromatic compounds as sole carbon and energy sources for growth. The degradation of aromatic compounds has been studied extensively in bacteria and fungi (8, 24, 45), but little is known about the aromatic metabolism by Archaea, which represents a third domain of life phylogenetically distinct from Bacteria and Eucarya (53). The *Hf.* D1227 metabolism of 3-phenylpropionic acid, which is a central metabolite in plant physiology (25), was studied to understand the archaeal strategies for phenylpropanoid catabolism.

Since cinnamic acid, benzoic acid, 3-hydroxybenzoic acid and gentisic

acid were detected in *Hf.* D1227 cultures grown on 3-phenylpropionic acid, it was hypothesied that 3-phenylpropionic acid was metabolized by β-oxidation of the side chain to benzoic acid, which was subsequently degraded via a gentisate pathway. The *Hf.* D1227 gentisate 1,2-dioxygenase, one of the key enzymes in the 3-phenylpropionic acid degradation pathway, was purified and characterized as a study of the first ring-fission dioxygenase from an extreme halophile. The gene encoding *Hf.* D1227 gentisate 1,2-dioxygenase was cloned and sequenced to obtain the first gentisate 1,2-dioxygenase gene sequence and information on the relationship between this archaeal gentisate 1,2-dioxygenase and other ring-cleavage dioxygenases.

Background

I. Archaea as a third domain of life

Haloferax sp. D1227 used in this study is a halophilic archaeon. It was twenty years ago when Carl Woese first announced his discovery of the Archaea - a group of organisms so different from all other living organisms, that he placed them in a separate domain of life (54). By comparison of

ribosomal RNA sequences, Woese articulated the now-recognized three primary lines of evolutionary descent, termed domains: Eucarya, Bacteria, and Archaea (53). A universal phylogenetic tree is shown in Figure 1.1. Within the archaeal domain, there are two taxonomic divisions (Euryarchaeota and Crenarchaeota) and three phenotypic groups, the methanogens, extreme thermophiles, and extreme halophiles. Among characteristics typical of Archaea are: (1) membrane lipids composed of ether-linked isoprenyl phosphoglycerides; (2) lack of muramic acid-containing peptidoglycan in the cell envelope; (3) the "common arm" of the RNAs contains pseudouridine or 1-methylpseudouridine instead of ribothymidine; and (4) the sequences of 5S, 16S, and 23S rRNA differ significantly from those of eubacteria and eucaryotes (29).

It is becoming clear that the three fundamental cellular information processing systems of Archaea - DNA replication, transcription and translation - are more similar to their eucaryotic than their bacterial counterparts (42). Archaeal DNA polymerases and replication fork proteins are eucaryote-like; bacteria and archaea-eucaryotes replication fork proteins

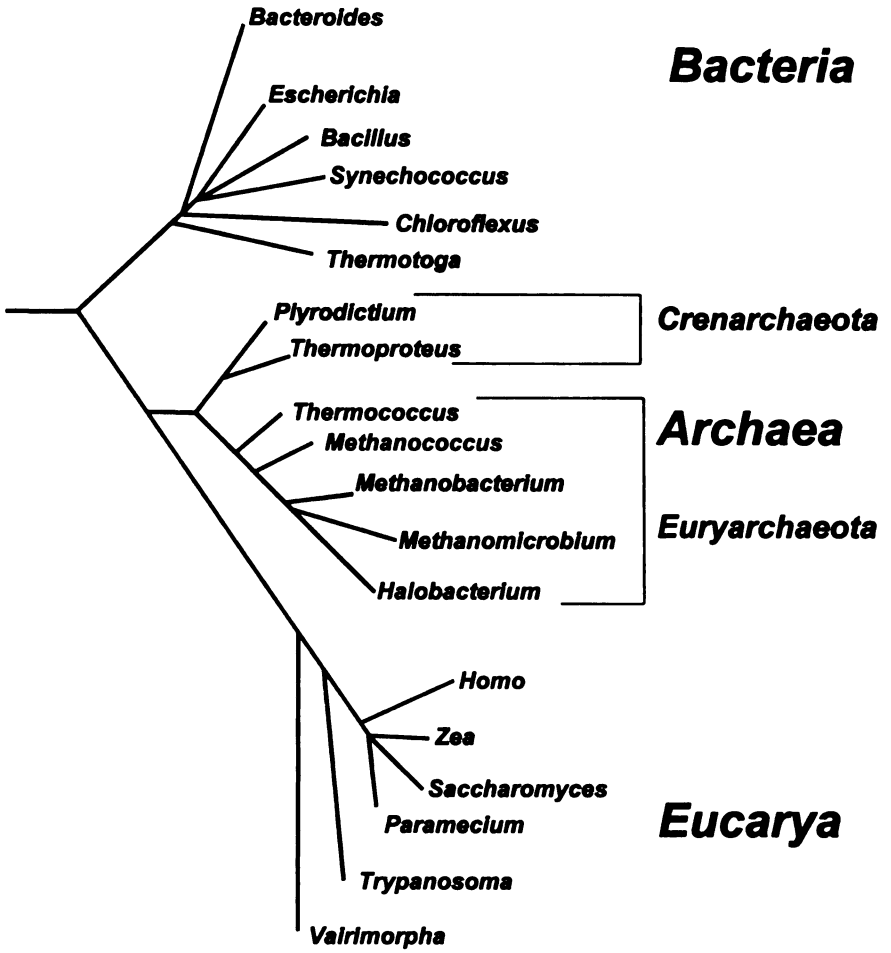

Figure 1.1 A universal phylogenetic tree based on small subunit ribosomal RNA sequences. The tree has been rooted by analysis of duplications in protein sequences. (Adapted from Olsen and Woese, 1997)

have little or no sequence similarity (21). In addition to the universally-distributed three largest subunits of the RNA polymerase, the archaeal RNA polymerase contains additional small subunits not found in the simpler bacterial enzyme, but all having counterparts in the eucaryotic version (33, 57). The transcription initiation system in Archaea is a simpler version of that seen in eucaryotes and basically different from the bacterial system (34, 57). The archaeal ribosomal proteins and tRNA charging enzymes are more similar to their eucaryotic than to their bacterial homologs (2).

Archaea also resemble Eucarya in many other aspects. Introns have been found in archaeal rRNAs and tRNAs, but not in mRNAs; and RNA splicing in Archaea resembles that of eucaryotes (23). One distinction between Eucarya and Bacteria is the presence of histones in Eucarya. Archaeal histones have been found which compact DNA into histone-DNA complexes analogous to the eucaryotic nucleosome, and sequence comparison shows that the eucaryotic and the archaeal histones evolved from the same ancestor (2).

The similarity of the fundamental information processing systems in Archaea (DNA replication, transcription, and translation) to their eucaryotic

counterparts and other resemblances between Archaea and Eucarya (RNA splicing, histones, etc.) strongly suggest that Archaea are more closely related to Eucarya than to Bacteria. However, the bacterial features in Archaea should not be overlooked. Archaea and Bacteria are quite similar in morphology, lack of nuclei, genomic organization, and metabolic pathways. Like Bacteria, Archaea have single circular chromosomes and genes are organized in operons; some archaeal operons are identical in gene order to bacterial operons (21). Archaeal metabolic genes in many key pathways such as carbon fixation, biosynthesis of amino acid, nucleotide, and coenzyme, are strikingly similar to bacterial counterparts (43).

The recently obtained first archaeal genome sequence from *Methanococcus jannaschii* provides valuable information on Archaea (7). A striking feature of the *M. jannaschii* genome is that about 50% of the potential coding sequences match no sequence in the databases, indicating the uniqueness of Archaea. Open reading frames encoding eucaryote-like DNA polymerase, replication proteins and DNA repair enzymes were detected in the genome of *M. jannaschii*. Ten of the eleven translation initiation factors, two of the three elongation factors, and the only release

factor recognized in *M. jannaschii* genome are of the eucaryotic type. In the *M. jannaschii* genome, genes for subunits of a complex such as RNA polymerase and ribosome are linked in an operon.

II. Overview of extremely halophilic, aerobic Archaea

Haloferax sp. D1227 used in this study is an extremely halophilic, aerobic archaeon. There are six recognized genera of halophilic Archaea, four genera of non-alkalophilic halophiles (i.e. *Halobacterium*, *Halococcus*, *Haloferax*, and *Haloarcula*) and two genera of alkalophilic halophiles (i.e. *Natronobacterium* and *Natronococcus*). Non-alkalophilic halophiles have been isolated from a variety of highly saline environments, including salted food products (fish, hides, bacon, and sausage), salt lakes such as the Great Salt Lake in Utah, the Dead sea, and hypersaline soils. In contrast, alkalophilic halophiles have mainly been found in highly alkaline soda lakes such as the Wadi Natrun in Egypt and Lake Magadi in Kenya. These halophiles are usually of a bright red-orange color due to the synthesis of bacterioruberin pigment, which protects the organisms against bright sunlight present at most habitats of extreme halophiles. The cell shapes of

halophilic Archaea, which are rods, cocci, square-shaped, or pleiomorphic, can vary depending on the growth conditions.

The optimum NaCl concentrations for the growth of extreme halophiles is typically between 2.6 M and 4.3 M. Some can even grow in saturated NaCl concentration (6 M). Na^+ and Cl^- ions are required for growth, but Na^+ can be partially replaced by K^+. Isolates from high Mg^{2+} environments such as the Dead Sea usually have high requirements of Mg^{2+}. Haloalkalophilic strains require a pH around 8.5 to 9.5, while the optimal range for nonalkalophilic halophiles is between pH 7 to 7.5. All halophilic Archaea grow well at 37 to 40 °C. Oxygen supply is an important parameter to consider in cultivating extreme halophiles, since the high salt concentrations decrease the oxygen solubility in the media. While *H. halobium* and related strains grow primarily on amino acids, *Haloferax* and *Haloarcula* species show the ability to use carbohydrates as carbon and energy sources. Some *Halobacterium* strains produce bacteriorhodopsin and are therefore capable of using sunlight as an energy source. In general, these organisms do not grow rapidly, exhibiting generation times 2 to 12 hours. Halophilic Archaea are highly resistant to most antibiotics.

To balance the high osmotic pressure and ionic strength in the hypersaline environments, extremely halophilic Archaea accumulate high concentrations of KCl inside the cells (9), unlike halophilic Bacteria and Eucarya where compatible solutes such as glycine and betaine are accumulated as osmotica. The high concentrations of intracellular KCl, approximately the concentration of NaCl in the medium, are deleterious to many common proteins and other biological macromolecules. High KCl causes aggregation of proteins because of enhancement of hydrophobic interactions, it interferes with electrostatic interaction because of charge shielding, and it reduces the availability of free water because of salt ion hydration (although K^+ hydrates less water than Na^+) (35). By introducing additional acidic residues (glutamic acid and aspartic acid) into the proteins, halophilic Archaea proteins are highly adapted to function in a milieu containing 2 to 5 M KCl. The bulk protein of the extreme halophiles contains an excess acidic over basic amino acids of close to 10%, whereas the bulk protein of the non-halophilic organisms is about chemically neutral (48). The X-ray crystal structures of halophilic malate dehydrogenase and 2Fe-2S ferredoxin (19, 22) show that most of the acidic residues are located

on the surfaces of the proteins. These acidic residues are more highly hydrated than other amino acids and can coordinate a hydrated salt ion network at the protein-solvent interface as demonstrated in crystals of halophilic ferredoxin. Acidic amino acids can also be used to form internal salt bridges with strategically-positioned basic residues inside the protein to provide structural rigidity. Excess acidic residues also reduce protein hydrophobicity. Comparison of halophilic archaeal protein-encoding genes with their nonhalophilic homologs exhibit an inordinately high proportion of nonsynonymous nucleotide substitutions, and many of the resulting amino acid replacements involve the addition, removal, relocation, or rearrangment of acidic residues (17).

Proteins from extreme halophiles are not only stable in high concentrations of salt, but actually require them for their function. Thus, purification of halophilic proteins requires procedures that can be carried out in the presence of high concentrations of salt such as gel filtration, hydroxyapatite, hydrophobic, and sulfate-mediated chromatography. Procedures that take place at low salt concentrations such as ion exchange chromatography can be effective only if inactivation can be reversed.

Enzymes purified to date from extreme halophiles include glutamine synthetase, superoxide dismutase, α-amylase, peroxidase, and ketohexokinase (5, 32, 37, 39, 46).

Unlike Bacteria characterized by a single cell wall polymer, the murein, Archaea exhibit a variety of non-murein polymers with remarkable structural and chemical diversity (51). In contrast to the ester linkage-based bacterial and eucaryotic lipids, archaeal core lipids are isopra(e)nyl glycerol ethers, and all lipids in Archaea contain a 2,3-*sn*-glycerol and C_{20}-C_{20}, C_{20}-C_{25} or C_{25}-C_{25} diethers (31). The polar lipids of halophilic Archaea are phospholipids and glycolipids.

Comparison of the central metabolism (i.e. conversion of hexose sugars to pyruvate, and then to CO_2 and H_2O via the citric acid cycle) in Archaea, Bacteria, and Eucarya suggests that the basic central pathways were established before the divergence of the three domains, with variations occurring thereafter (16). Halophilic archaeal membranes possess typical components of bacterial respiratory system including flavoproteins, quinones and cytochromes of types *a*, *b*, *c*, and *o*; the only difference being that a high salt concentration is required for maintaining structure and

function of the respiratory chain in extreme halophiles (26).

The genomes of halophilic Archaea are similar in size to those of Bacteria, both chromosomes and widely distributed plasmids are circular. The G+C content of the bulk of the DNA is > 60 mol% and total DNA can be separated into two fractions according to G+C content in most cases. Chromosomal sequences of 62 to 71 mol% G+C constitute the major fraction, whereas the more A + T rich minor fraction (55 to 58 mol% G+C) consists mainly of covalently closed circular DNAs (cccDNA). The genomic instability of *Halobacterium halobium* due to insertion elements is not a common feature of all halophilic Archaea (44).

Genetics in extreme halophiles is still in the early stage. Bi-directional genetic exchange has been demonstrated in *H. volcanii* which requires cell-cell contact, but no cell fusion occurring (40). Polyethylene glycol (PEG) mediated spheroplast transformation of halophilic Archaea has been successful in transforming plasmids and linear genomic DNA, as well as phage DNA transfection (10). Shuttle vectors with selective markers (mevinolin and novobiocin) which can replicate in both *H. volcanii* and *E. coli* have been developed (28, 36). Transposons with selectable marker

genes have also been constructed, although no natural transposons have been detected in Archaea (18). With these useful tools, a modest number of halophilic archaeal genes has been characterized including genes encoding rRNAs, ribosomal proteins, bacteriorhodopsin, halorhodopsin, gas-vesicle proteins, and superoxide dismutase (4, 30, 38, 41, 49). A consensus TTA(A/T) sequence for the archaeal promoters is usually located 27±4 bp upstream from the translation start codon (57). It has been calculated that *Methanococcus jannaschii* uses initiation codons ATG, GTG, and TTG about 70%, 25%, and 5% of the time respectively (7). All halophilic rRNA operons seem to share a common 16S-23S-5S gene organization reminiscent of that found in eubacteria (41).

III. Aerobic degradation of phenylpropanoids by microorganisms

Degradation of the aromatic compound 3-phenylpropionic acid by *Haloferax* sp. D1227 was the focus of this study. As aromatic compounds with aliphatic side chains, phenylpropanoids present microorganisms with a choice as to their mode of attack. One choice is to undergo hydroxylation of the aromatic ring prior to degradation of the side chain as demonstrated

in a species of *Achromobacter* and two strains of *Pseudomonas* (3, 11, 15). Another is shortening of side chains first via a mechanism similar to fatty acid β-oxidation cycle as suggested by Webley et al. (50) based on whole cell experiments, but not enzyme studies. The fatty acid β-oxidation pathway (Figure 1.2) is usually induced by growth on oils, fatty acids or alkanes. After entering the cells via various mechanisms, fatty acids are first activated to acyl-CoA thioesters by chain length-specific acyl-CoA synthetases prior to their oxidative degradation. In the following acyl-CoA dehydrogenase reaction, one molecule of FAD, which is often tightly bound to the bacterial and mitochondrial enzymes, is reduced and reoxidized through the electron transfer chain yielding ATP; whereas the peroxisomal enzyme is a flavin enzyme in which the flavin is reoxidized by oxygen directly producing H_2O_2. After the 2,3-enoyl-CoA hydratase step, another dehydrogenase reaction is carried out by NAD^+-dependent 3-hydroxyacyl-CoA dehydrogenase. The generated NADH is linked to oxidative phosphorylation in bacteria and mitochondria, and to glycerol-3-phosphate dehydrogenase in the peroxisomes. The final reaction of the cycle involves the CoA-dependent cleavage of the acyl chain by 3-ketoacyl-CoA thiolase

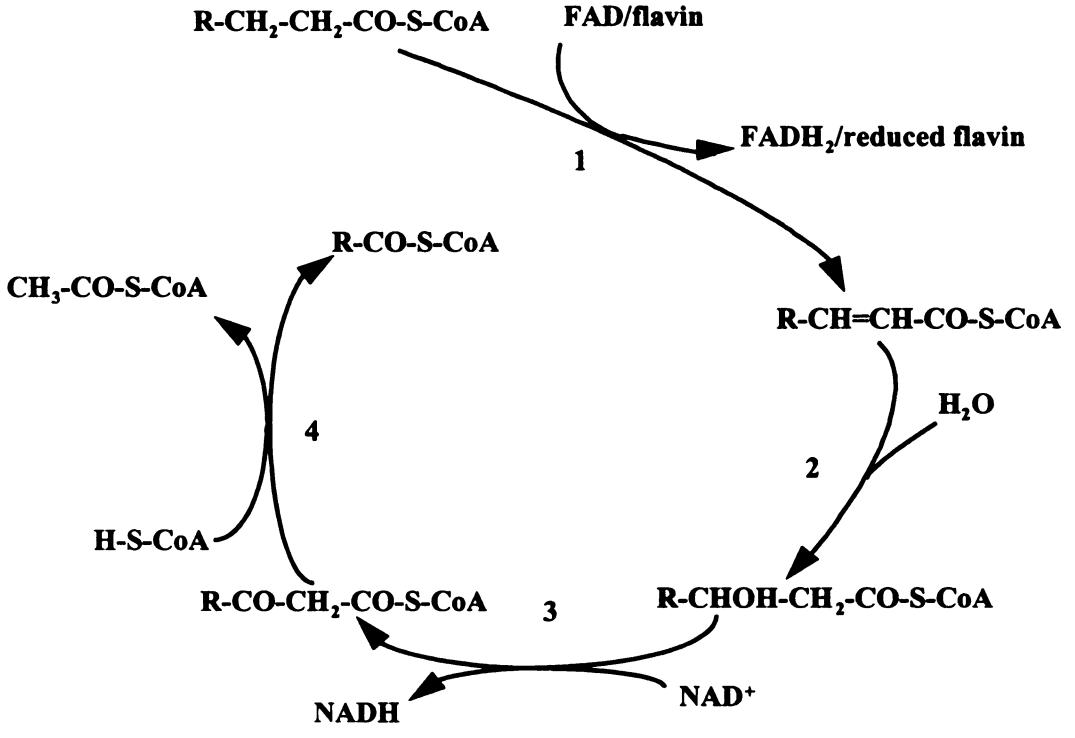

Figure 1.2 Fatty acid β-oxidation cycle. Individual enzyme reactions: 1. Fatty acyl-CoA dehydrogenase; 2. 2,3-enoyl-CoA hydratase; 3. 3-hydroxyacyl-CoA dehydrogenase; 4. 3-ketoacyl-CoA thiolase. (Adapted from Ratledge, 1994)

resulting in a two carbon shorter fatty acyl-CoA molecule, which reenters the cycle without further activation (47). Although in mitochondria, all enzymes of the β-oxidation appear as separable, mono-function proteins, there is a remarkable degree of structural organization in the bacterial and peroxisomal enzymes (56).

After scission of the aliphatic side chains, the resulting aromatic compounds are usually transformed by monooxygenases and dioxygenases into central intermediates such as catechol, protocatechuate and gentisate before ring cleavage (24). It is generally accepted that dihydroxylation is a prerequisite for enzymatic fission of the aromatic ring, which renders the aromatic ring more reactive to electrophilic attack (27). A number of different pathways for transforming benzoic acid into the dihydroxylated intermediates have been demonstrated (Figure 1.3). As shown in pathway1, some species such as *Alcaligenes eutrophus* and *Pseudomonas arvilla* metabolize benzoate to catechol by benzoate 1,2-dioxygenase, a two-component ring-hydroxylating dioxygenase. One component is the NAD(P)H reductase containing a FAD and a [2Fe-2S] redox center and the second component is the terminal dioxygenase in an $(\alpha\beta)_3$ configuration

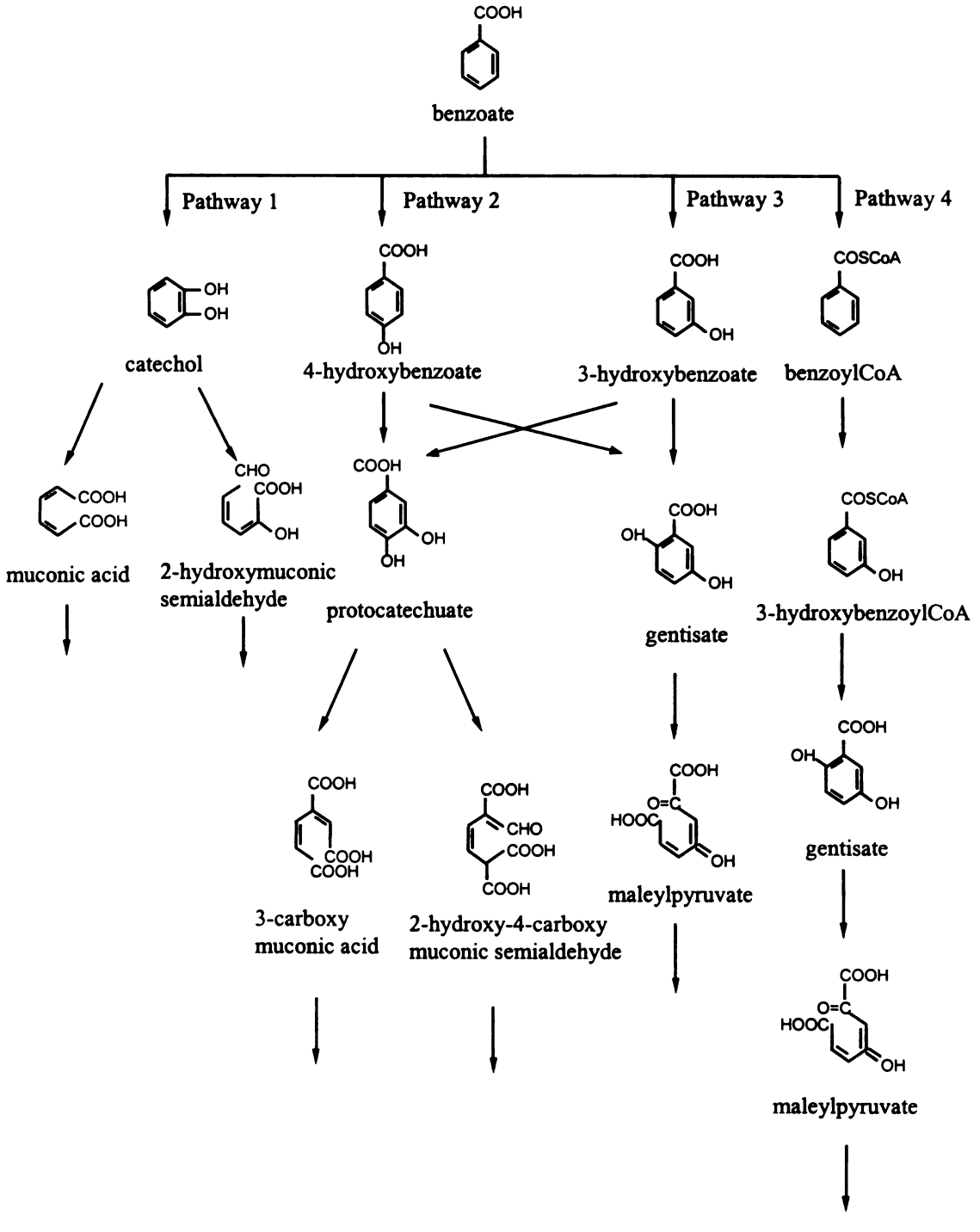

Figure 1.3 Aerobic benzoate degradation pathways in various microorganisms.

(55). Pathway 2 and 3 were demonstrated in some members of *Pseudomonas*, *Streptomyces* and *Bacillus* where benzoate was metabolized to gentisate or protocatechuate via either 3- or 4-hydroxybenzoate (12, 13). 4-Hydroxybenzoate-3-hydroxylase and 3-hydroxybenzoate-6-hydroxylase involved in these two pathways have been studied in detail, both are single-component flavoproteins with NAD(P)H as external electron donors (27, 52). Recently, Altenschmidt et al. (1) proposed a fourth benzoate degradation pathway involving CoA derivatives. Their research shows that a facultative denitrifying *Pseudomonas* strain KB740 metabolizes benzoate aerobically via benzoylCoA and 3-hydroxybenzoylCoA rather than via free acids, and 3-hydroxybenzoylCoA is further degraded via gentisate. The aerobic benzoate-CoA ligase in this pathway is not closely related to its anaerobic counterpart based on immunological comparison. The activity of the purified benzoylCoA-3-monooxygenase is dependent on a flavin nucleotide (FAD or FMN), NADPH, and benzoylCoA. Although the involvement of CoA thioesters in the anaerobic degradation of aromatic compounds is well known, only a few reports have described aerobic pathways with CoA derivatives as intermediates, i.e. the metabolism of 2-

aminobenzoate and the dehalogenation of 4-halobenzoate (6, 14). The authors postulated that one reason for utilizing CoA thioesters in aerobic metabolism is that the degradation of naturally abundant C_6-C_3 compounds by β-oxidation results in benzoylCoA and analogues, and it is advantageous to metabolize these compounds directly since free aromatic acids are membrane-permeable. The dihydroxylated aromatic ring of the central intermediates are opened by ring-cleavage dioxygenases leading to intermediates of the tricarboxylic acid cycle (8).

References

1. Altenschmidt, U., B. Oswald, E. Steiner, H. Herrmann, and G. Fuchs. 1993. New aerobic benzoate oxidation pathway via benzoyl-coenzymeA and 3-hydroxybenzoyl-coenzymeA in a denitrifying *Pseudomonas*. J. Bacteriol. 175: 4851-4858.

2. Amils, R., P. Cammarano, and P. Londei. 1993. Translation in archaea. 393-438. In: M. Kates et al. (ed.), The biochemistry of Archaea (Archaebacteria). Elsevier Science Publishers, New York.

3. Blakley, E. R. and F. J. Simpson. 1964. The microbial metabolism of cinnamic acid. Can. J. Microbiol. 10: 175-185.

4. Blanck, A., and D. Oesterhelt. 1987. The halo-opsin gene. II. Sequence, primary structure of halorhodopsin and comparison with bacteriohodopsin. EMBO J. 6: 265-273.

5. Brown-Peterson, N. J., and M. L. Salin. 1993. Purification of a catalase-peroxidase from *Halobacterium halobium*: characterization of some unique properties of the halophilic enzyme. J. Bacteriol. 175: 4197-4202.

6. Buder, R., and G. Fuchs. 1989. 2-Aminobenzoyl-CoA monooxygenase/reductase, a novel type of flavoenzyme. Purification and some properties of the enzyme. Eur. J. Biochem. 185: 637-643.

7. Venter, J. C., C. J. Bult, O. White, G. J. Olsen, L. Zhou, R. D. Fleischmann, G. G. Sutton, J. A. Blake, L. M. FitzGerald, R. Clayton, J. D. Gocayne, C. I. Reich, R. Overbeek, E. F. Kirkness, K. G. Weinstock, J. M. Merrick, A. Glodek, J. L. Scott, N. S. M. Geoghagen, J. F. Weidman, J. L. Fuhrmann, M. C. Hanna, M. D. Cotton, K. M. Roberts, M. A. Hurst, B. P. Kaine, M. Borodovsky, H. Klenk, C. M. Fraser, H. O. Smith, C. R. Woese, A. R. Kerlavage, B. A. Dougherty, J. Tomb, M. D. Adams, D. Nguyen, T. R. Utterback, J. M. Kelley, J. R. Peterson, P. W. Sadow. 1996. Complete genome sequence of the methanogenic archaeon, *Methanococcus jannaschii*. Science. 273: 1058-1073.

8. Cain, R. B. 1980. The uptake and catabolism of lignin-related aromatic compounds and their regulation in microorganisms. 21-56. In: T. K. Kirk et al. (ed.), Lignin biodegradation: microbiology, chemistry, and potential applications. CRC press, Inc., Florida.

9. Christian, J. H. B., and J. A. Waltho. 1962. Solute concentrations within cells of halophilic and non-halophilic bacteria. Biochem. Biophys. Acta. 65: 506-508.

10. Cline, S. W., W. L. Lam, R. L. Charlebois, L. C. Schalkwyk, and W. F. Doolittle. 1989. Transformation methods for halophilic archaebacteria. Can. J. Microbiol. 35: 148-152.

11. Coulson C. B., and W. C. Evans. 1959. Microbiological degradation of trans-cinnamic acid by soil *Pseudomonads*. Chem. & Ind. 543-544.

12. Crawford, R. L. 1975. Degradation of 3-hydroxybenzoate by bacteria of the genus *Bacillus*. Appl. Microbiol. 30: 439-444.

13. Crawford, R. L. 1976. Pathways of 4-hydroxybenzoate degradation among species of *Bacillus*. J. Bacteriol. 127: 204-210.

14. Crooks, G. P., and S. D. Copley. 1993. A surprising effect of leaving group on the nucleophilic aromatic substitution reaction catalyzed by 4-chlorobenzoyl-CoA dehalogenase. J. Am. Chem. Soc. 115: 6422-6423.

15. Dagley, S., P. J. Chapman, and D. T. Gibson. 1965. The metabolism of β-phenylpropionic acid by an *Achromobacter*. Biochem. J. 97: 643-650.

16. Danson, M. J. 1993. Central metabolism of the archaea. 1-24. In: M. Kates et al. (ed.), The biochemistry of Archaea (Archaebacteria). Elsevier Science Publishers, New York.

17. Dennis, P. P., and L. C. Shimmin. 1997. Evolutionary divergence and salinity-mediated selection in halophilic archaea. Microbiol. Mol. Biol. Rev. 61: 90-104.

18. Dyall-Smith, M. L., and W. F. Doolittle. 1994. Construction of composite transposons for halophilic Archaea. Can. J. Microbiol. 40: 922-929.

19. Dym, O., M. Mevarech, and J. L. Sussman. 1995. Structural features that stabilize halophilic malate dehydrogenase from an archaebacterium. Science. 267: 1344-1346.

20. Emerson, D., S. Chauhan, P. Oriel, and J. A. Breznak. 1994. *Haloferax* sp. D1227, a halophilic Archaeon capable of growth on aromatic compounds. Arch. Microbiol. 161: 445-452.

21. Forterre, P., and C. Elie. 1993. Chromosome structure, DNA topoisomerases, and DNA polymerases in archaebacteria (archaea). 325-365. In: M. Kates et al. (ed.), The biochemistry of Archaea (Archaebacteria). Elsevier Science Publishers, New York.

22. Frolow, F., M. Harel, J. L. Sussman, M. Mevarech, and M. Shoham. 1996. Insights into protein adaptation to a saturated salt environment from

the crystal structure of a halophilic 2Fe-2S ferredoxin. Nat. Struct. Biol. 3: 452-458.

23. Garrett, R. A., C. Aagaad, M. Anderson, J. Z. Dalgaard, J. Lykke-Anderson, H. T. N. Phan, S. Trevisanato, L. Ostergaard, N. Larsen, and H. Leffers. 1994. Archaeal rRNA operons, intron splicing and homing endonucleases, RNA polymerase operons and phylogeny. System. Appl. Microbiol. 16: 680-691.

24. Gibson, D. T. and V. Subramanian. 1984. Microbial degradation of aromatic hydrocarbons. 181-252. In: D. T. Gibson (ed.), Microbial degradation of organic compounds. Marcel Dekker Inc., New York.

25. Hahlbrock, K., and D. Scheel. 1989. Physiology and molecular biology of phenylpropanoid metabolism. Annu. Rev. Plant Physiol. Plant Mol. Biol. 40: 347-369.

26. Hallberg, G. C., and A. Colmsjo. 1989. Four different b-type cytochromes in the halophilic archaebacterium *Halobacterium halobium*. Arch. Biochem. Biophys. 272: 130-136.

27. Harayama, S., and M. Kok. 1992. Functional and evolutionary relationships among diverse oxygenases. Annu. Rev. Microbiol. 46: 565-601.

28. Holmes, M. L., and M. L. Dyall-Smith. 1990. A plasmid vector with a selectable marker for halophilic archaebacteria. J. Bacteriol. 172: 756-761.

29. Holt, J. G., N. R. Kieg, P. H. A. Sneath, J. T. Sraley, and S. T. Williams. 1993. Bergey's manual of determinative bacteriology. Ninth edition. p. 12. Williams & Wilkins. Baltimore.

30. Horne, M., C. Englest, and F. Pfeifer. 1988. Two gas vacuole proteins in *Halobacterium halobium*. Mol. Gen. Genet. 213: 59-464.

31. Kamekura, M., and M. Kates. 1988. Lipids of halophilic archaebacteria. Vol. 2: 25-65. In: F. Rodriguez-Valera (ed.), Halophilic bacteria. CRC Press, Inc., Florida.

32. Kobayashi, T., H. Kanai, T. Hayashi, T. Akiba, R. Akaboshi, and K. Horikoshi. 1992. Haloalkaliphilic maltotriose-forming α-amylase from the archaebacterium *Natronococcus* sp. Strain Ah-36. J. Bacteriol. 174: 3439-3444.

33. Langer, D., J. Hain, P. Thuriaux, and W. Zillig. 1995. Transcription in archaea: similarity to that in Eucarya. Proc. Natl. Acad. Sci. USA. 92: 5768-5772.

34. Nikolov, D. B., and S. K. Burley. 1997. RNA polymerase II transcription initiation: a structural view. Proc. Natl. Acad. Sci. USA. 94: 15-22.

35. Lanyi, J. K. 1974. Salt-dependent properties of proteins from extremely halophilic bacteria. Bacteriol. Rev. 38: 272-290.

36. Lam, W. L., and W. F. Doolittle. 1989. Shuttle vectors for the archaebacterium *H. Volcanii*. Proc. Natl. Acad. Sci. USA. 86: 5478-5482.

37. Manitz, B., and A. W. Holldorf. 1993. Purification and properties of glutamine synthetase from the archaebacterium *Halobacterium salinarium*. Arch. Microbiol. 159: 90-97.

38. May, B. P., P. Tam, and P. P. Dennis. 1990. The expression of the superoxide dismutase gene in *Halobacterium cutirubrum* and *H. volcanii*. Can. J. Microbiol. 35: 171-175.

39. May, B. P., and P. P. Dennis. 1987. Superoxide dismutase from the extremely halophilic archaebacterium *Halobacterium cutirubrum*. J. Bacteriol. 169: 1417-1422.

40. Mevarech, M., and R. Werczberger. 1985. Genetic transfer in *Halobacterium volcanii*. J. Bacteriol. 162: 461-462.

41. Mevarech, M., S. Hirsch-Twizer, S. Goldman, E. Yakobson, H. Eisenberg, and P. P. Dennis. 1989. Isolation and characterization of the rRNA gene clusters of *Halobacterium marismortui.* J. Bacteriol. 171: 3479-3485.

42. Olsen, G. J., and C. R. Woese. 1997. Archaeal genomics: an overview. Cell. 89: 991-994.

43. Olsen, G. J., and C. R. Woese. 1996. Lessons from an Archaeal genome: what are we learning from *Methanococcus jannaschii*? Trends. Genet. 12: 377-379.

44. Pfeifer, F. 1988. Genetics of halobacteria. Vol. 2: 105-133. In: F. Rodriguez-Valera (ed.), Halophilic bacteria. CRC Press, Inc., Florida.

45. Rochkind, M. L., J. W. Blackburn, and G. S. Sayler. 1987. Metabolism of non-chlorinated compounds. 45-68. In: M. L. Rochkind et al. (ed.), Microbial decomposition of chlorinated aromatic compounds. U. S. Environmental Protection Agency, Cincinnati, Ohio.

46. Rangaswamy, V., and W. Altekar. 1994. Ketohexokinase (ATP: D-fructose 1-phosphotransferase) from a halophilic archaebacterium, *Haloarcular vallismortis*: purification and properties. J. Bacteriol. 176: 5505-5512.

47. Ratledge, C. 1994. Biodegradation of oils, fats and fatty acids. 89-141. In: C. Ratledge (ed.), Biochemistry of microbial degradation. Kluwer academic publishers, Netherlands.

48. Reistad, R. 1970. On the composition and nature of the bulk protein of the extremely halophilic bacteria. Arch. Microbiol. 71: 353-360.

49. Shimmin, L., and P. P. Dennis. 1989. Characterization of the L11, L1, L10 and L12 equivalent ribosomal protein gene cluster of the halophilic archaebacteria *Halobacterium cutirubrum.* EMBO J. 8: 1225-1235.

50. Webley, D. M., R. B. Duff, and V. C. Farmer. 1955. Beta-oxidation of fatty acids by *Nocardia opaca.* J. Gen. Microbiol. 13: 361-369.

51. Wieland, F. 1988. The cell surfaces of halobacteria. Vol. 2: 55-65. In: F. Rodriguez-Valera (ed.), Halophilic bacteria. CRC Press, Inc., Florida.

52. Wierenga, R. K., K. H. Kalk, J. M. van der laan, J. Drenth, J. Hofsteenge, W. J. Weijer, P. A. Jekel, J. J. Beintema, F. Muller, and W. J. H. van Berkel. 1982. The structure of *p*-hydroxybenzoate hydroxylase. 11-19. In V. Massey et al. (ed.), Flavins and flavoproteins. Elsevier Science Publishers, New York.

53. Woese, C. R., O. Kandler, and M. L. Wheelis. 1990. Toward a natural system of organisms: proposal for the domains Archaea, Bacteria, and Eucarya. Proc. Natl. Acad. Sci. USA. 87: 4576-4579.

54. Woese, C. R., and G. E. Fox. 1977. Phylogenetic structure of the procaryotic domain: the primary kingdoms. Proc. Natl. Acad. Sci. USA. 74: 5088-5090.

55. Yamaguchi, M., and H. Fujisawa. 1982. Subunit structure of oxygenase component in benzoate 1,2-dioxygenase system from *Pseudomonas arvilla* C-1. J. Biol. Chem. 257: 12497-12502.

56. Yang, S. Y., and H. Schulz. 1983. The large subunit of the fatty acid oxidation complex from *Escherichia coli* is a multifunctional polypeptide. J. Biol. Chem. 258: 9780-9785.

57. Zillig, W., P. Palm, H. Klenk, D. Langer, U. Hudepohl, J. Hain, M. Lanzendorfer, and I. Holz. 1993. Transcription in archaea. 367-391. In: M. Kates et al. (ed.), The biochemistry of Archaea (Archaebacteria). Elsevier Science Publishers, New York.

Chapter 2

DEGRADATION OF 3-PHENYLPROPIONIC ACID BY *HALOFERAX* SP. D1227

Abstract

Haloferax sp. D1227, isolated from soil contaminated with highly saline oil brine, is the first halophilic archaeon to demonstrate the utilization of aromatic compounds (i.e., 3-phenylpropionic acid, cinnamic acid and benzoic acid) as sole carbon and energy sources for growth. The degradation of 3-phenylpropionic acid in this strain was studied to examine the strategies utilized by Archaea to metabolize aromatic compounds. Based on the following findings: (1) the extracellular accumulation of cinnamic acid, benzoic acid, 3-hydroxybenzoic acid, and gentisic acid in cultures of *Hf.* D1227 grown on 3-phenylpropionic acid; (2) the presence of an 3-phenylpropionylCoA dehydrogenase; (3) the ATP, CoA and NAD-dependent conversion of cinnamic acid to benzoylCoA; and (4) the presence of gentisate 1,2-dioxygenase, we propose that *Hf.* D1227 metabolizes

3-phenylpropionic acid by initial 2-carbon shortening of the side chain to benzoylCoA via a mechanism similar to fatty acid β-oxidation, followed by aromatic degradation using a gentisate pathway. The upper aliphatic pathway from 3-phenylpropionic acid to benzoic acid is separately regulated from the lower gentisate pathway.

Introduction

Haloferax sp. D1227, isolated from soil contaminated with highly saline oil brine near Grand Rapids, Michigan, is a halophilic archaeon requiring 2 M NaCl for optimal growth. To date, *Hf.* D1227 is the only reported archaeon capable of aerobic metabolism of aromatic compounds (i.e., benzoic acid, cinnamic acid, and 3-phenylpropionic acid) as sole carbon and energy sources for growth (12). Although the pathways for degradation of aromatic compounds in bacteria and fungi have been elucidated in detail (5, 13, 25), little is known about the aromatic catabolism by Archaea. Since the recognition that Archaea, consisting of methanogens, extreme thermophiles and extreme halophiles, represents a third domain of life phylogenetically distinct from Bacteria and Eucarya (33), biochemical and genetic research has elucidated some unusual features of these organisms and provided new

insights into their evolutionary relationships with bacterial and eucaryotic organisms (11, 18, 24). The isolation of *Hf.* D1227 provides an opportunity to investigate the strategies utilized by Archaea for catabolism of aromatic compounds and to compare an aromatic degradation pathway in Archaea with those in Bacteria and Eucarya.

3-Phenylpropionic acid is a member of the phenylpropanoid family comprising a wide variety of C_6-C_3 compounds synthesized by plants from phenylalanine. Phenylpropanoids are important in plant physiology for synthesis of lignin, flavonoids, insect repellents, UV protectants, and signal molecules (15). It has been shown that the microbial degradation of 3-phenylpropionic acid can occur via two different routes. In one route demonstrated in a species of *Achromobacter* and two strains of *Pseudomonas* (2, 6, 9), the aromatic ring is first oxidized and opened, followed by the degradation of the resulting aliphatic segment. An alternative route for the degradation of 3-phenylpropionic acid is catabolism of the side chain followed by aromatic ring fission. This latter pathway was suggested by Webley et al. (30) based on their observation of the transient accumulation of cinnamic acid and benzoic acid by *Nocardia opoca* grown

with 3-phenylpropionic acid. They proposed that 3-phenylpropionic acid was metabolized by two carbon shortening of the side chain first, via a mechanism similar to fatty acid β-oxidation, resulting in benzoylCoA. The enzymes involved in this oxidation were not investigated, nor was the degradation of benzoylCoA. Under aerobic conditions, benzoate is usually transformed into a few key intermediates including catechol, protocatechuate and gentisate, followed by aromatic ring cleavage by ring-fission dioxygenases (13). Recently, Altenschmidt et al. (1) demonstrated a new aerobic benzoate degradation pathway involving CoA derivatives. Their research showed that *Pseudomonas* KB740, a facultative denitrifying *Pseudomonas* species, metabolized benzoate to 3-hydroxybenzoylCoA via benzoylCoA with further 5-hydroxylation to gentisate.

In this paper, we present results which indicate that the degradation of 3-phenylpropionic acid by *Hf.* D1227 is initiated by β-oxidation of the side chain to produce benzoylCoA, which is subsequently metabolized via a gentisate pathway.

Materials and Methods

Materials. All chemicals used in this study were reagent grade. 3-phenylpropionic acid, cinnamic acid and benzoic acid were purchased from Aldrich Chemical Co. (Milwaukee, WI.). Catechol, protocatechuic acid, gentisic acid, salicylic acid, 3-hydroxybenzoic acid, 4-hydroxybenzoic acid, oleic acid, lauric acid, palmitic acid, Triton X-100, ATP, CoenzymeA and 2,2'-dipyridyl were obtained from Sigma chemical Co. (St. Louis, MO.). HPLC grade acetonitrile was purchased from EM Science (Gibbstown, NJ.).

Microorganism, media, and growth conditions. *Haloferax* sp. D1227 has been described (12). For growth of *Hf.* D1227 on various carbon sources, mineral salts medium (BS3) (12) of the following composition (in g/l) was used: $(NH_4)_2SO_4$, 0.33; KCl, 6.0; $MgCl_2 \cdot 6H_2O$, 12.1; $MgSO_4 \cdot 7H_2O$, 14.8; KH_2PO_4, 0.34; $CaCl_2 \cdot H_2O$, 0.36; and NaCl, 100. 1 ml/l of a trace element solution (32) was also added prior to sterilization and the pH was adjusted to 6.9 with KOH. Filter-sterilized growth substrates were added after sterilization. For rich medium (BSYT), BS3 mineral salts medium was supplemented with 3 g/l yeast extract and 3 g/l tryptone. For solid media, 15 g/l Bacto-agar was added prior to autoclaving. Cells were

cultured aerobically in Erlenmeyer flasks containing 1/4 volume of BS3 mineral salt medium supplemented with various growth substrates. For growth on fatty acids, the sole carbon source was 1 mM oleic acid, lauric acid, or palmitic acid with or without 0.4% (v/v) Triton X-100 to disperse fatty acids (34). Each flask was inoculated with a mid-log phase culture grown in BSYT rich medium to give an initial OD_{600nm} approximately 0.02. Flasks were incubated at 37°C on a rotary shaker at 200 rpm. Growth was monitored by measuring OD_{600nm} on a Gilford DU spectrophotometer except that growth on fatty acids was determined by viable count plating.

HPLC analysis. Aromatic compounds were analyzed by reverse-phase HPLC on a Waters model chromatography (Waters, Millipore Corp., Milford, Mass.) equipped with a Waters 486 tunable absorbance detector set at 254nm, a Waters 746 integrator and Waters model 501 solvent delivery system. Separation was achieved on a Nova-Pak™ C18 column (150×3.9 mm) at a flow rate of 0.8 ml/min. The injection volume was 20 µl. Free aromatic acids were eluted using 2% acetonitrile in 200 mM ammonium acetate buffer (pH 6.5). CoA thioesters were eluted using 15% acetonitrile in 200 mM ammonium acetate buffer (pH 5.5). For CoA derivatives for

which standards were unavailable, 3 μl of 10N NaOH was added to 300 μl samples to hydrolyze CoA thioesters to their corresponding free acids (31). Aromatic acids, benzoylCoA, and 3-hydroxybenzoylCoA were identified by comparison of retention times with those of authentic standards.

Resting cell experiments with added 2,2'-dipyridyl. Cells grown on 3 mM 3-phenylpropionic acid, cinnamic acid, benzoic acid, or pyruvate were harvested when the culture (250 ml) reached mid-log phase at an OD_{600nm} of approximately 0.7. Following centrifugation at 10,600×*g* for 30 min, cells were washed twice with 100 mM potassium phosphate buffer (pH 7.0) containing 2 M KCl and resuspended in 25 ml of the same buffer. Each 125 ml Erlenmeyer flask contained in a total volume of 10 ml: 100 mM potassium phosphate buffer (pH 7.0) containing 2 M KCl, 4 ml of the cell suspension, 5 mM 2,2'-dipyridyl, and 1 mM 3-phenylpropionic acid, cinnamic acid, benzoic acid, or 3-hydroxybenzoic acid. Cells were incubated at 37°C on a rotary shaker at 200 rpm. Samples were filtered through 0.2 μm nylon filters (Scientific Resources Inc., Eatontown, NJ.), and analyzed immediately by HPLC.

Preparation of cell-free extracts. *Hf.* D1227 was grown in 250 ml BS3 medium containing 3 mM 3-phenylpropionic acid, cinnamic acid, benzoic acid or pyruvate. Cells in mid-log phase were harvested by centrifugation at 10,600×*g* for 30 min, washed twice with 30 ml 100 mM potassium phosphate buffer (pH 7.0) containing 2 M KCl, and resuspended in 10 ml of the same buffer. Using a 4710 Series Ultrasonic Homogenizer (Cole-Parmer Instrument Co., Chicago, IL.), 2.5 ml aliquots of the suspension were sonicated four times (30 seconds at 50 W followed by 2 min of cooling) in an ice bath. Unbroken cells and cell debris were removed by ultracentrifugation (245,300×*g* for 1 hour at 4 °C). The supernatants were then diafiltrated using Centricon-10 (MW cut-off : 10,000. Amicon, Inc., Beverly, MA.) at 4°C with three volumes of 100 mM potassium phosphate buffer (pH 7.0) containing 2 M KCl to remove small molecules in the extracts. The concentrated extracts were diluted with the same buffer to 10 ml for enzyme analysis.

Enzyme assays. All enzyme assays were performed at 37°C, unless stated otherwise. **3-Phenylpropionic acid-CoA ligase, cinnamic acid-CoA ligase, benzoic acid-CoA ligase, and 3-hydroxybenzoic acid-CoA**

ligase. The assay mixture for ligase activity contained in a total volume of 0.5 ml: 100 mM potassium phosphate buffer (pH 7.0) containing 2 M KCl, 0.5 mM 3-phenylpropionic acid, cinnamic acid, benzoic acid or 3-hydroxybenzoic acid, 2 mM ATP, 2 mM Coenzyme A, 10 mM $MgCl_2$ and 50 µl of cell-free extract. The ligase activities were determined by measuring the rate of the appearance of CoA thioester products using HPLC.

3-PhenylpropionylCoA dehydrogenase. In order to assay 3-phenylpropionylCoA dehydrogenase activity, 3-phenylpropionylCoA, which is not commercially available, was synthesized from 3-phenylpropionic acid with *Hf.* D1227 cell-free extracts utilizing the 3-phenylpropionic acid-CoA ligase reaction described above. Since the reaction catalyzed by 3-phenylpropionylCoA dehydrogenase required no added cofactor, cinnamylCoA started to appear in the ligase reaction mixture upon the formation of 3-phenylpropionylCoA. The 3-phenylpropionylCoA dehydrogenase activity was determined by measuring the rate of cinnamylCoA production using HPLC.

Conversion of cinnamylCoA to benzoylCoA. Since cinnamylCoA is not commercially available, it was synthesized from cinnamic acid with *Hf.* D1227 cell-free extracts utilizing cinnamic acid-CoA ligase reaction described above. Once the formation of cinnamylCoA ceased, NAD was added to the reaction mixture (0.5 ml) to a final concentration of 1 mM to initiate the conversion of cinnamylCoA to benzoylCoA. The simultaneous disappearance of cinnamylCoA and appearance of benzoylCoA were measured using HPLC.

BenzoylCoA-3-hydroxylase, 3-hydroxybenzoylCoA-6-hydroxylase, benzoate-3-hydroxylase, and 3-hydroxybenzoate-6-hydroxylase. BenzoylCoA-3-hydroxylase, 3-hydroxybenzoylCoA-6-hydroxylase, benzoate -3-hydroxylase, and 3-hydroxybenzoate-6-hydroxylase activities were assayed using the methods modified from those described by Niemetz et al.(23), Kiemer et al. (19), Wang et al. (29), Suarez et al. (26), van Berkel et al. (27), and Groseclose et al. (14). The reaction mixture in a total volume of 1 ml contained: 100 mM potassium phosphate buffer (pH 7.0) containing 2 M KCl, or 100 mM Tris-HCl buffer (pH 7.0) containing 2 M KCl; 0.25 mM benzoylCoA, 3-hydroxybenzoylCoA, benzoate, or

3-hydroxybenzoate; 0.1 mM NADH or NADPH or in combination with 0.1 mM FAD; 200 µl supernatant or resuspended pellet of sonicated or 0.1% Triton X-100 treated cells. The stabilizers, 0.1 mM DTT, 0.1% glycerol, and 0.1 mM EDTA, were also added to the reaction mixture, either individually or in combination. The enzyme activities were determined by measuring the appearance of hydroxylation products on HPLC.

Gentisate 1,2-dioxygenase. Gentisate 1,2-dioxygenase was assayed at room temperature by measuring the formation of maleylpyruvate at 334 nm (20) with a Perkin Elmer double beam 124 spectrophotometer. The reaction mixture (2 ml) contained 0.25 mM gentisic acid, 50 µl cell-free extract, and 100 mM potassium phosphate buffer (pH 7.0) containing 2 M KCl. The reference cuvette contained the same reaction mixture except gentisic acid was omitted. The molar absorption coefficient for maleylpyruvate (ε = 10,800) (7) was used to calculate enzyme activity. This assay was confirmed by measurement of the disappearance of gentisate using HPLC.

***cis-trans* Isomerase.** Since maleylpyruvate is not commercially available, it was synthesized from gentisic acid by gentisate 1,2-dioxygenase as described above. When the formation of maleylpyruvate

ceased, glutathione was added to the reaction mixture to a final concentration of 1 mM. The activity of *cis-trans* isomerase was determined by measuring the disappearance of maleylpyruvate at 334 nm (20).

Protein determination. Protein concentrations of crude enzyme extracts were determined by the method of Bradford (3) with bovine serum albumin dissolved in 100 mM potassium phosphate buffer (pH 7.0) containing 2 M KCl as the standard.

Nucleotide sequence analysis of small-subunit (SSU) rDNA. To prepare genomic DNA of *Hf.* D1227, cells were grown in 100 ml BSYT medium and harvested at mid-log phase by centrifugation at 10,600×*g* for 30 min. After washing twice with 100 mM potassium phosphate buffer (pH 7.0) containing 2 M KCl, the pellet was resuspended in 50 ml distilled water for cell lysis. After removal of cell debris by centrifugation at 47,800×*g* for 30 min, the supernatant was extracted once with an equal volume of phenol, and twice with an equal volume of phenol/chloroform. DNA in the aqueous phase was precipitated with 2 volumes of ethanol and 0.1 volume of 3 M sodium acetate (pH 5.2) at −16°C overnight. After centrifugation, the pellet was rinsed with 1 ml of 70% ethanol, air dried, and resuspended in 1 ml of

H_2O (22). This preparation was then treated with RNase at a final concentration of 25 μg/ml and used as template DNA for PCR. The PCR reaction mixture in a total volume of 100 μl contained: 2 μl of template DNA (ca. 100 ng), 20 mM Tris-HCl (pH 8.4), 50 mM KCl, 1.5 mM $MgCl_2$, 0.25 mM of each dNTP, 2.5 U of *Taq* DNA polymerase, and 30 pmol of each primer. Primers ARCH21BF [5'-TCCGCTTGATCC(C/T)GCC(A/G) G-3'] and 1492R [5'-GGTTACCTTGT TACGACTT-3'] have been described (21). PCR reaction was carried out on Perkin Elmer GeneAmp PCR System 2400 (Perkin Elmer, Norwalk, CT.) and thermal cycling conditions were 94°C for 5 min followed by 35 cycles of 94°C for 30 sec, 55°C for 45 sec, and 72°C for 2.1 min. A final extension was performed at 72°C for 6.1 min. PCR product was purified with GENECLEAN II Kit (BIO 101 Inc., La Jolla, CA.) following the protocol recommended by the manufacturer. Nucleotide sequencing was carried out at the Nucleic Acid Sequencing Facility of Michigan State University with an ABI Prism sequencer (Applied Biosystems). The following sequencing primers were used: ARCH 21BF, 269R [5'-TACCGAT TATCGGCACGGTG-3'], 356F [5'-AGGCGCGAAAC CTT TACACT-3'], 592F [5'-CGAAGGTTCATCGG

GAAATC-3'], 960R [5'-ATGTCCGGCGTT GAGTCCA A-3'], 1196R [5'-ATTCGGGGCATACTG ACCTA-3'], 1352F[5'-CGCATTTCAATAGAGT GCGG-3'], and 1492R. An edited, contiguous sequence was constructed from the data manually. A list of the known sequences that were most similar to the SSU rRNA sequence of *Hf.* D1227 was obtained using the "Similarity Rank" routine at the Ribosomal Database Project (University of Illinois, Urbana-Champaign). Sequences were then aligned manually with Genome database Environment version 2.2 operating on a Sun SPARC station. Similarity matrix was constructed with the Jukes and Cantor correction for base changes. Phylogenetic trees were constructed from the same alignment by distance and maximum-parsimony methods (the later was bootstrapped with SEQBOOT). These analyses were run with PHYLIP version 3.55c.

RESULTS

Small-subunit (SSU) rRNA sequence analysis. To confirm the earlier identification of *Hf.* D1227 as a *Haloferax* species (12), the small subunit rRNA encoding gene from *Hf.* D1227 was amplified by PCR using

Archaea-specific forward primer ARCH21BF and "universal" reverse primer 1492R. Sequence corresponding to *E. coli* SSU rRNA nucleotide position 26 through 1491 was obtained. *Hf.* D1227 showed 98.4% and 98.2% sequence similarities to *Haloferax volcanii* and *Haloferax mediterranei* respectively. The unrooted phylogenetic tree constructed by maximum-parsimony analysis grouped *Hf.* D1227 within the genus *Haloferax*, and this grouping was supported by bootstrap value of 100% for the node from which this strain and the other members of the genus radiate (Figure 2.1). The distance method also grouped *Hf.* D1227 within the genus *Haloferax* (tree not shown). Out of the 26 nucleotide differences between *Hf.* D1227 and its closest relative *Hf. volcanii*, there were four dual-compensatory differences corresponding to *E. coli* positions 128 and 233, 141 and 222, 184 and 191, 835 and 851.

Aerobic growth of *Hf.* D1227 on aromatic compounds and fatty acids. In addition to growth on 3-phenylpropionic acid, cinnamic acid and benzoic acid previously described (12), *Hf.* D1227 also demonstrated the ability to utilize 3-hydroxybenzoic acid (1 mM) as a sole carbon source. No growth was observed with 4-hydroxybenzoic acid (1 mM), salicylic acid (1 mM),

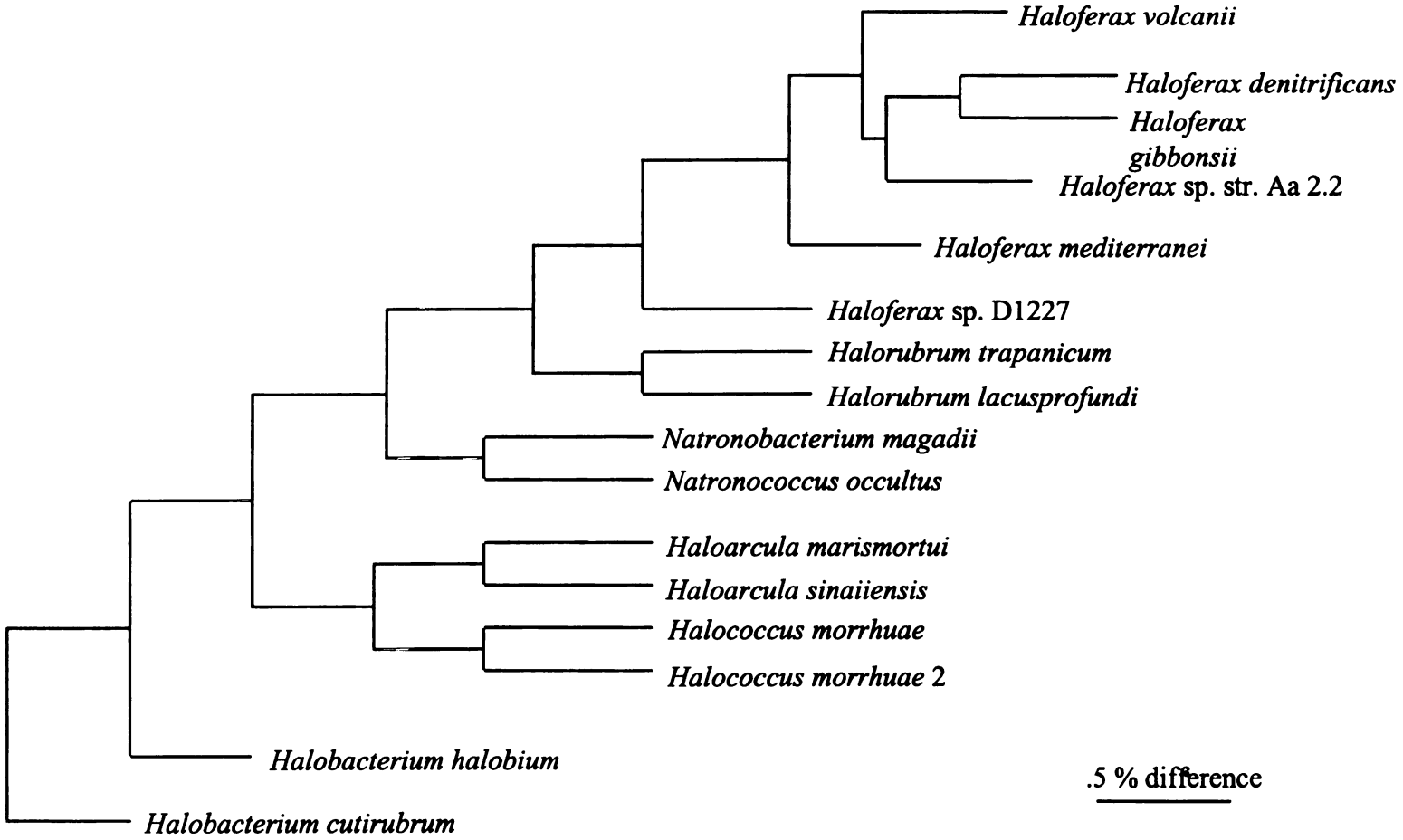

Figure 2.1 Phylogenetic position of strain D1227 within the genus *Haloferax* based on a maximum-parsimony analysis. The bar represents a 0.5% difference in evolutionary distance.

catechol (0.1 mM), protocatechuic acid (0.1 mM), gentisic acid (0.1 mM), oleic acid (1 mM), lauric acid (1 mM), and palmitic acid (1 mM). Lack of growth on gentisic acid was attributed to the inhibitory effect of either gentisic acid or its autoxidation products, since growth of *Hf.* D1227 on benzoate was inhibited when gentisic acid was added to the medium.

The metabolites detected by HPLC analysis in the cultures of *Hf.* D1227 grown on 3 mM 3-phenylpropionic acid, cinnamic acid, or benzoic acid (Table 2.1) suggested that cinnamic acid, benzoic acid, 3-hydroxybenzoic acid and gentisic acid were intermediates in 3-phenylpropionic acid degradation.

Resting cell experiments with added 2,2'-dipyridyl. To observe metabolites detected during growth in more detail, resting cell experiments were carried out with added 2,2'-dipyridyl, which is an inhibitor of gentisate 1,2-dioxygenase (See **enzyme activities**), thus blocking further degradation of gentisic acid. When 2,2'-dipyridyl and 3-phenylpropionic acid were incubated with resting cell suspensions of *Hf.* D1227 pregrown on 3-phenylpropionic acid, accumulations of the following metabolites were observed (in the order of decreasing concentration): gentisic acid,

Table 2.1 Aromatic metabolites observed in 48 hour *Hf.* D1227 cultures grown on various substrates.

Growth substrate (3mM)	Aromatic metabolites observed in 48 hour culture	Concentration (μM)
3-phenylpropionic acid	cinnamic acid	0.061
	benzoic acid	0.048
	3-hydroxybenzoic acid	0.079
	gentisic acid	0.035
cinnamic acid	benzoic acid	0.086
	3-hydroxybenzoic acid	0.095
	gentisic acid	0.074
benzoic acid	3-hydroxybenzoic acid	0.104
	gentisic acid	0.073
pyruvate	none	/

3-hydroxybenzoic acid, benzoic acid, and cinnamic acid (Figure 2.2). The detection of these metabolites in high concentrations provided additional evidence that *Hf.* D1227 metabolized 3-phenylpropionic acid via cinnamic acid, benzoic acid, 3-hydroxybenzoic acid and gentisic acid. When the intermediates involved in the 3-phenylpropionic acid degradation pathway and 2,2'-dipyridyl were added to 3-phenylpropionic acid-grown cell suspension, the anticipated metabolites from the proposed pathway were seen, i.e. benzoic acid, 3-hydroxybenzoic acid and gentisic acid accumulated when cinnamic acid was added as the substrate; 3-hydroxybenzoic acid and gentisic acid accumulated with benzoic acid as the substrate; gentisic acid accumulated with 3-hydroxybenzoic acid as the substrate (data not shown).

Enzyme activities. The following enzyme activities were found in the soluble fraction of *Hf.* D1227 cells. **3-Phenylpropionic acid-CoA ligase, cinnamic acid-CoA ligase, benzoic acid-CoA ligase, and 3-hydroxy benzoic acid-CoA ligase**. Crude extracts prepared from cells grown on 3-phenylpropionic acid demonstrated ATP and CoA-dependent ligase activities which converted 3-phenylpropionic acid, cinnamic acid, benzoic

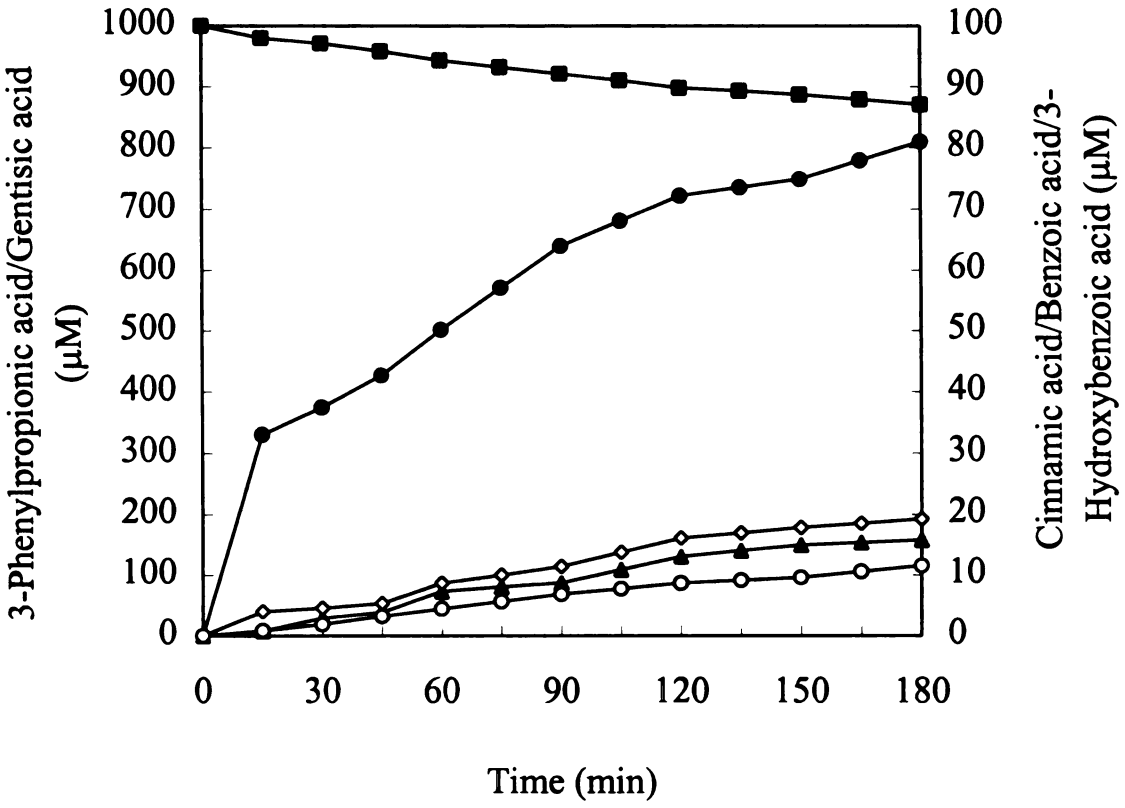

Figure 2.2 Accumulation of intermediates when 3-phenylpropionic acid and 2,2'-dipyridyl were added to 3-phenylpropionic acid-grown cells

- 3-phenylpropionic acid
- cinnamic acid
- benzoic acid
- 3-hydroxybenzoic acid
- gentisic acid

acid, and 3-hydroxybenzoic acid to their corresponding CoA derivatives. Stimulation of ligase activities was observed with the addition of 10 mM $MgCl_2$ to the reaction mixtures (Table 2.2). These ligase activities were also detected in cells grown on cinnamic acid, benzoic acid, or pyruvate. It is not yet known whether these reactions are catalyzed by the same ligase or different ones, and also whether they are constituous or inducible.

3-PhenylpropionylCoA dehydrogenase. The activity of 3-phenylpropionylCoA dehydrogenase catalyzing the conversion of 3-phenylpropionylCoA to cinnamylCoA was present in extracts of 3-phenylpropionic acid-grown cells with a specific activity of 526±19 nmol cinnamylCoA produced/min·mg protein and also in extracts of cinnamic acid-grown cells with a specific enzyme activity of 711±24 nmol cinnamylCoA produced /min·mg protein. This enzyme activity was not detectable in cells grown on benzoic acid or pyruvate. The reaction catalyzed by the 3-phenylpropionylCoA dehydrogenase proceeded without any added cofactor. When 1 mM FAD, NAD, or NADP was added to the reaction mixture, only FAD addition stimulated enzyme activity (50%). No conversion of 3-phenylpropionic acid to cinnamic acid was observed

Table 2.2 Stimulation effect of $MgCl_2$ on ligase activity

Ligase	Specific enzyme activity (μM thioester product/min·mg protein)		Stimulation (fold)
	0 mM $MgCl_2$	10 mM $MgCl_2$	
3-Phenylpropionic acid-CoA ligase,	1.9±0.3	7.3±0.9	3.5
cinnamic acid-CoA ligase	1.1±0.2	6.7±0.7	6.0
benzoic acid-CoA ligase	3.6±0.5	15.8±0.4	4.0
3-hydroxybenzoic acid-CoA ligase	0.4±0.05	1.0±0.07	2.5

Note: Crude extracts prepared from 3-phenylpropionic acid-grown *Hf.* D1227 cells were used in this experiment.

without both ATP and Coenzyme A added to the reaction mixture. Flushing the reaction mixture with nitrogen gas caused 34 % loss of enzyme activity, suggesting the possible involvement of O_2 in the reaction. Since 3-phenylpropionylCoA dehydrogenase activity was demonstrated only in the soluble fraction of *Hf.* D1227, membrane-associated electron transfer proteins appear not to be involved in this dehydrogenation reaction.

Conversion of cinnamylCoA to benzoylCoA. Conversion of cinnamylCoA to benzoylCoA was observed with cell-free extracts prepared from cells grown on either 3-phenylpropionic acid, or cinnamic acid. This conversion was NAD-dependent over a broad concentration range with maximal conversion at 1 mM NAD (Figure 2.3). NADP and FAD were ineffective. Extracts of benzoic acid or pyruvate-grown cells did not show the ability to transform cinnamylCoA to benzoylCoA, and no conversion of cinnamic acid to benzoic acid was detected without both ATP and Coenzyme A added to the reaction mixture.

BenzoylCoA-3-hydroxylase, 3-hydroxybenzoylCoA-6-hydroxylase, benzoate-3-hydroxylase, and 3-hydroxybenzoate-6-hydroxylase. BenzoylCoA, 3-hydroxybenzoylCoA, benzoate and 3-hydroxybenzoate

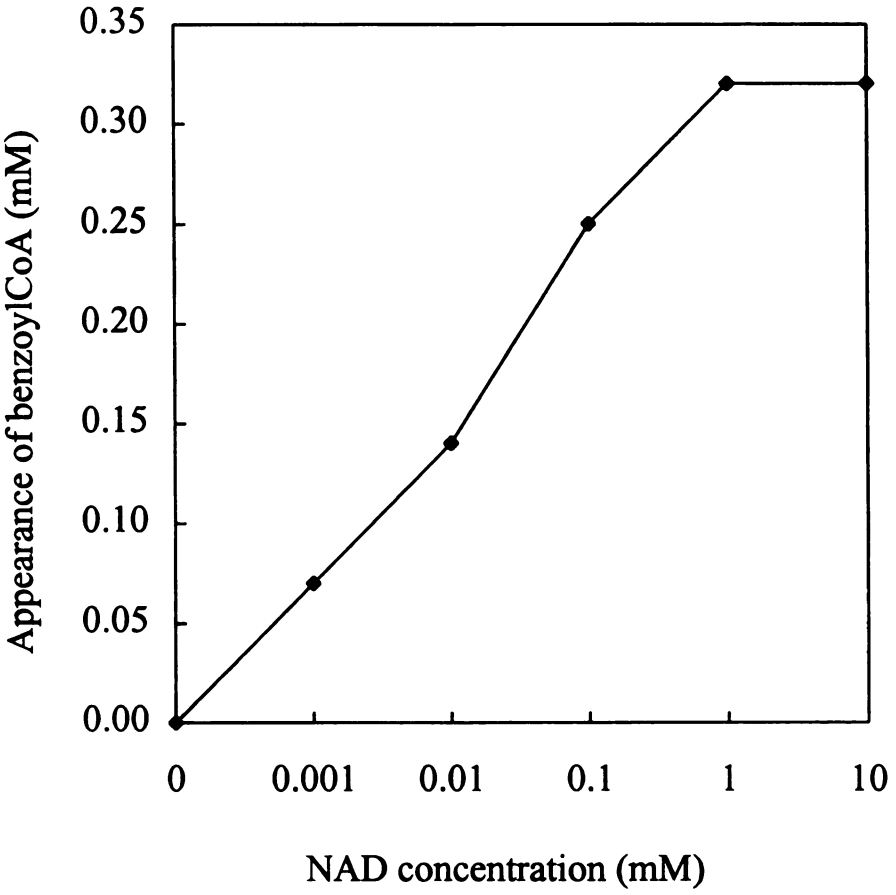

Figure 2.3 Effect of NAD on the conversion of cinnamylCoA to benzoylCoA

hydroxylation enzymes were not detected using the assay methods described in **Materials and Methods** in cells grown on 3-phenylpropionic acid, cinnamic acid, or benzoic acid.

Gentisate 1,2-dioxygenase. Gentisate 1,2-dioxygenase activity was demonstrated in extracts from cells grown with 3-phenylpropionic acid, cinnamic acid, or benzoic acid with a specific activity of 1.4±0.2, 1.5±0.3, or 1.2±0.3 μmol maleylpyruvate produced/min·mg protein respectively. This enzyme activity was not detectable in pyruvate-grown cells. Unlike reported eubacterial gentisate 1,2-dioxygenases (7, 16, 19), no stimulating effect of Fe^{2+} on enzyme activity was observed, although 2,2'-dipyridyl was an inhibitor for the enzyme activity (Figure 2.4). The optimal salt concentration for the activity was 2 M KCl or NaCl. Detailed studies of the purified gentisate 1,2-dioxygenase and its encoding gene will be presented in chapter 3.

cis-trans **Isomerase.** A glutathione-dependent *cis-trans* isomerase with a specific activity of 47.6±3.9 μmol/min ·mg protein was present in cells grown on benzoic acid. When the ring fission reaction of gentisate catalyzed by gentisate 1,2-dioxygenase ceased, the reaction mixture showed

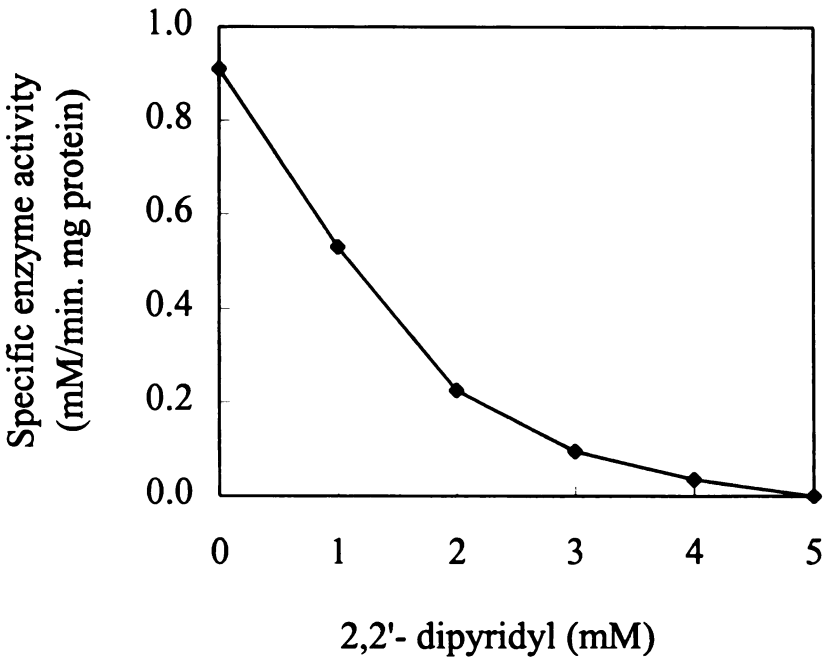

Figure 2.4 Inhibition of gentisate 1,2-dioxygenase activity by 2,2'-dipyridyl

a product peak at 334 nm corresponding to the absorption maximum of maleylpyruvate. A rapid decrease of the 334 nm absorbance was observed when 1 mM glutathione was added to the mixture. This was attributed to the presence of a *cis-trans* isomerase which interconverts maleylpyruvate and fumarylpyruvate upon the addition of glutathione (20).

Pathway induction. To study the induction of the 3-phenylpropionic acid degradation pathway, 2,2'-dipyridyl and suspensions of *Hf.* D1227 resting cells pregrown on 3-phenylpropionic acid, cinnamic acid, benzoic acid, or pyruvate were incubated with 3-phenylpropionic acid or benzoic acid, and the appearance of metabolites in the culture was examined. When 3-phenylpropionic acid and 2,2'-dipyridyl were incubated with suspension of cells pregrown with either 3-phenylpropionic acid or cinnamic acid, metabolites of 3-phenylpropionic acid degradation were detected in the culture. However, when either a pyruvate or benzoic acid-grown cell suspension was used, no metabolites of 3-phenylpropionic acid degradation were detected (Table 2.3). When benzoic acid and 2,2'-dipyridyl were added to suspensions of cells grown on pyruvate or benzoic acid, 3-hydroxybenzoic acid and gentisic acid accumulated in benzoic acid-grown

Table 2.3 Accumulation of intermediates when 3-phenylpropionic acid and 2,2'-dipyridyl were added to cells pregrown on various substrates

Growth substrate (3mM)	Accumulation of intermediates in 3 hours (μM)			
	cinnamic acid	benzoic acid	3-hydroxy benzoic acid	gentisic acid
3-phenylpropionic acid	1.6±0.3	1.9±0.2	8.1±1.2	115±14
cinnamic acid	0.5±0.07	2.9±0.4	52.5±3.3	317±26
benzoic acid	0	0	0	0
pyruvate	0	0	0	0

cells, but not in pyruvate-grown cells (data not shown). These data indicate that the upper aliphatic pathway from 3-phenylpropionic acid to benzoic acid can be induced by either 3-phenylpropionic acid or cinnamic acid, but not benzoate. The lower gentisate pathway from benzoic acid to gentisic acid is induced by benzoate.

Discussion

Although the extracellular metabolites observed during growth and in resting cell experiments suggest aerobic metabolism of 3-phenylpropionic acid via cinnamic acid, benzoic acid, 3-hydroxybenzoic acid, and gentisic acid, the enzyme data indicate its catabolism via CoA thioesters, which are not released extracellularly due to membrane impermeability. The presence of thioesterase activities converting 3-phenylpropionylCoA, cinnamylCoA, benzoylCoA, and 3-hydroxybenzoylCoA to their corresponding free acids was demonstrated in *Hf.* D1227 cells grown on 3-phenylpropionic acid, cinnamic acid, benzoic acid or pyruvate (data not shown). The accumulation of benzoic acid in the cultures of *Hf.* D1227 grown on 3-phenylpropionic acid suggests that 2-carbon scission of the

3-phenylpropionic acid side chain resulting in benzoic acid precedes attack on the aromatic nucleus. The enzyme results indicate that the transformation of 3-phenylpropionic acid to benzoic acid occurs via a mechanism similar to fatty acid β-oxidation. Although the anticipated but unstable intermediates 3-hydroxy-3-phenylpropionylCoA and 3-keto-3-phenylpropionylCoA (17) were not detected in the incubation of cinnamylCoA and NAD with cell-free extracts, NAD-dependent conversion of cinnamylCoA to benzoylCoA was observed.

The accumulation of 3-hydroxybenzoic acid and gentisic acid in benzoic acid-grown cells suggests that benzoic acid is converted to gentisic acid via 3-hydroxybenzoic acid. Although it is clear that gentisic acid serves as the substrate for gentisate 1,2-dioxygenase, we have not yet detected either benzoate or 3-hydroxybenzoate hydroxylase activity. Thus whether benzoic acid is transformed into gentisic acid via benzoylCoA and 3-hydroxy benzoylCoA as demonstrated by Altenschmidt et al. (1) or via free acids remains to be clarified. The proposed pathway for 3-phenylpropionic acid degradation in *Hf.* D1227 is shown in Figure 2.5.

The enzyme steps in the aliphatic pathway are separately regulated from

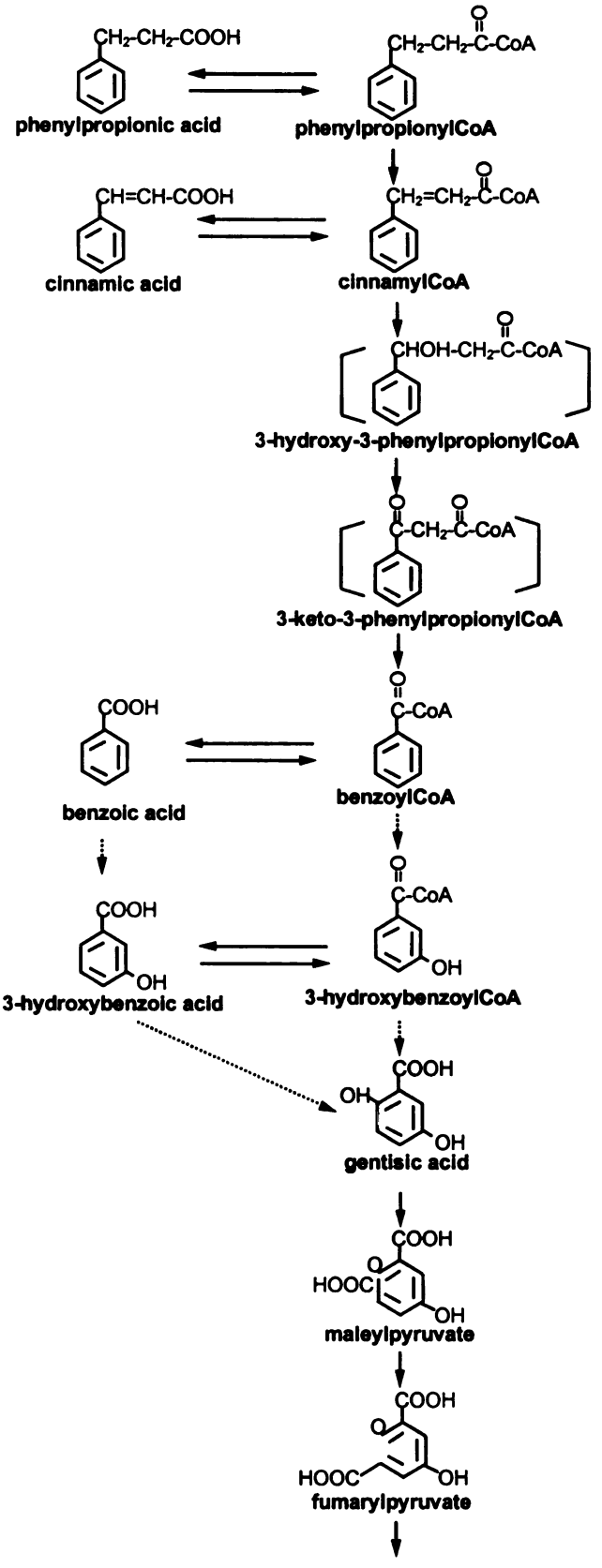

Figure 2.5 Proposed pathway for the degradation of 3-phenylpropionic acid by *Hf.* D1227

the aromatic gentisate pathway. Although the upper pathway steps strongly resemble those of fatty acid β-oxidation, their induction by phenylpropanoids (i.e. 3-phenylpropionic acid and cinnamic acid) and lack of fatty acid utilization by *Hf.* D1227 suggest that they are distinct.

While the importance of CoA thioesters in the anaerobic degradation of aromatic compounds has long been recognized (10), the involvement of CoA derivatives in aerobic aromatic pathways has only recently been described (1, 4, 8, 28). Our results indicate the participation of CoA thioesters in the 2-carbon shortening of the side chain of 3-phenylpropionic acid that had been postulated in eubacteria, but for which no enzyme activities have been described (30).

In summary, *Haloferax* sp. D1227 metabolizes 3-phenylpropionic acid by 2-carbon scission of the aliphatic side chain via a β-oxidation mechanism to produce benzoylCoA, which is further degraded via a gentisate pathway. Although lack of pathway details precludes in-depth comparisons, overall similarities between the *Hf.* D1227 pathway and that of eubacteria suggest the possibility of general pathway existence prior to the separation of Archaea and Bacteria.

Acknowledgments

We wish to thank Georg Fuchs for kindly providing 3-hydroxy benzoylCoA. We are extremely grateful to Mike Roberts and Jared Leadbetter for help with molecular phylogeny. We also thank Olga Maltseva, Tae-Kyou Cheong and David Emerson for many helpful discussions. This work was supported by AURIG from Michigan State University.

References

1. Altenschmidt, U., B. Oswald, E. Steiner, H. Herrmann, and G. Fuchs. 1993. New aerobic benzoate oxidation pathway via benzoyl-coenzymeA and 3-hydroxybenzoyl-coenzymeA in a denitrifying *Pseudomonas*. J. Bacteriol. 175: 4851-4858.

2. Blakley, E. R. and F. J. Simpson. 1964. The microbial metabolism of cinnamic acid. Can. J. Microbiol. 10: 175-185.

3. Bradford, M. M. 1976. A rapid and sensitive method for the quantitation of microgram quantities of protein utilizing the principle of protein-dye binding. Anal. Biochem. 72: 248-254.

4. Buder, R., and G. Fuchs. 1989. 2-Aminobenzoyl-CoA monooxygenase /reductase, a novel type of flavoenzyme. Purification and some properties of the enzyme. Eur. J. Biochem. 185: 637-643.

5. Cain, R. B. 1980. The uptake and catabolism of lignin-related aromatic compounds and their regulation in microorganisms. 21-56. In: T. K. Kirk

et al. (ed.), Lignin biodegradation: microbiology, chemistry, and potential applications. CRC press, Inc., Florida.

6. Coulson C. B., and W. C. Evans. 1959. Microbiological degradation of trans-cinnamic acid by soil *Pseudomonads*. Chem. & Ind. 543-544.

7. Crawford, R. L., S. W. Hutton, and P. J. Chapman. 1975. Purification and properties of gentisate 1,2-dioxygenase from *Moraxella osloensis*. J. Bacteriol. 121: 794-799.

8. Crooks, G. P., and S. D. Copley. 1993. A surprising effect of leaving group on the nucleophilic aromatic substitution reaction catalyzed by 4-chlorobenzoyl-CoA dehalogenase. J. Am. Chem. Soc. 115: 6422-6423.

9. Dagley, S., P. J. Chapman, and D. T. Gibson. 1965. The metabolism of β-phenylpropionic acid by an *Achromobacter*. Biochem. J. 97: 643-650.

10. Dangel, W., R. Barckman, A. Lack, M. Mohamed, J. Koch, B. Oswald, B. Seyfried, A. Tschech, and G. Fuchs. 1991. Differential expression of enzyme activities initiating anoxic metabolism of various aromatic compounds via benzoylCoA. Arch. Microbiol. 155: 256-262.

11. Darnell, J. E., and W. F. Doolittle. 1986. Speculations on the early cause of evolution. Proc. Natl. Acad. Sci. USA. 83: 1271-1275.

12. Emerson, D., S. Chauhan, P. Oriel, and J. A. Breznak. 1994. *Haloferax* sp. D1227, a halophilic Archaeon capable of growth on aromatic compounds. Arch. Microbiol. 161: 445-452.

13. Gibson, D. T. and V. Subramanian. 1984. Microbial degradation of aromatic hydrocarbons. 181-252. In: D. T. Gibson (ed.), Microbial degradation of organic compounds. Marcel Dekker Inc., New York.

14. Groseclose, E. E., and D. W. Ribbons. 1973. 3-Hydroxybenzoate 6-hydroxylase from *Pseudomonas aeruginosa*. Biochem. Biophys. Res. Commun. 55: 897-903.

15. Hahlbrock, K., and D. Scheel. 1989. Physiology and molecular biology of phenylpropanoid metabolism. Annu. Rev. Plant Physiol. Plant Mol. Biol. 40: 347-369.

16. Harpel, M. R., and J. D. Lipscomb. 1990. Gentisate 1,2-dioxygenase from *Pseudomonas*: purification, characterization and comparison of the enzymes from *Pseudomonas testosteroni* and *Pseudomonas acidovorans*. J. Biol. Chem. 265: 6301-6311.

17. Hilton, M. D., and W. J. Cain. 1990. Bioconversion of cinnamic acid to acetophenone by a *Pseudomonod*: microbial production of a natural flavor compound. Appl. Environ. Microbiol. 56: 623-627.

18. Juez, G. 1988. Taxonomy of extremely halophilic Archaebacteria. In: F. Rodriguez-Valera (ed.), Halophilic bacteria. CRC press, Inc., Florida.

19. Kiemer, P., B. Tshisuaka, S. Fetzer, and F. Lingens. 1996. Degradation of benzoate via benzoyl-coenzyme A and gentisate by *Bacillus stearothermophilus* PK1, and purification of gentisate 1,2-dioxygenase. Biol. Fertil. Soils. 23: 307-313.

20. Lack, L. 1959. The enzymic oxidation of gentisic acid. Biochem. Biophys. Acta. 34: 117-123.

21. Leadbetter, J. R., and J. A. Breznak. 1996. Physiological ecology of *Methanobrevibacter cuticularis* sp. nov. and *Methanobrevibacter curvatus* sp. nov., isolated from the hindgut of the termite *Reticulitermes flavipes*. Appl. Environ. Microbiol. 62: 3620-3631.

22. Maniatis, T., E. F. Fritsch, and J. Sambrook. 1982. Molecular cloning: a laboratory manual. Cold Spring Harbor Laboratory Press, Cold Spring Harbor, New York.

23. Niemetz, R., U. Altenschmidt, S. Brucker, G. Fuchs. 1995. Benzoyl-coenzyme-A 3-monooxygenase, a flavin-dependent hydroxylase. Purification, some properties and its role in aerobic benzoate oxidation via gentisate in a denitrifying bacterium. Eur. J. Biochem. 227: 161-168.

24. Olsen, G. J., and C. R. Woese. 1997. Archaeal genomics: an overview. Cell. 89: 991-994.

25. Rochkind, M. L., J. W. Blackburn, and G. S. Sayler. 1987. Metabolism of non-chlorinated compounds. 45-68. In: M. L. Rochkind et al. (ed.), Microbial decomposition of chlorinated aromatic compounds. U. S. Environmental Protection Agency, Cincinnati, Ohio.

26. Suarez, M., E. Ferrer, A. Garrido-Pertierra, and M. Martin. 1995. Purification and Characterization of the 3-hydroxybenzoate 6-hydroxylase from *Klebsiella pneumoniae*. FEMS Microbiol. Lett. 126: 283-290.

27. van Berkel, W. J. H., W. J. J. van den Tweel. 1991. Purification and characterization of 3-hydroxyphenylacetate 6-hydroxylase: a novel FAD-dependent monooxygenase from a *Flavobacterium* species. Eur. J. Biochem. 201: 585-592.

28. Vitovski, S. 1993. Phenylacetate-coenzyme A ligase is induced during growth on phenylacetic acid in different bacteria of several genera. FEMS Microbiol. Lett. 108: 1-6.

29. Wang, L-H., R. Y. Hamzah, Y. Yu, S-C. Tu. 1987. *Pseudomonas cepacia* 3-hydroxybenzoate 6-hydroxylase: induction, purification and characterization. Biochemistry. 26: 1099-1104.

30. Webley, D. M., R. B. Duff, and V. C. Farmer. 1955. Beta-oxidation of fatty acids by *Nocardia opaca*. J. Gen. Microbiol. 13: 361-369.

31. Webster, L. T., J. J. Mieyal, and U. A. Siddiqui. 1974. Benzoyl and hydroxybenzoyl esters of coenzyme A. Ultraviolet characterization and reaction mechanism. J. Biol. Chem. 249: 2641-2645.

32. Widdel, F., and F. Bak. 1992. Gram-negative mesophilic sulfate-reducing bacteria. 3342-3378. In: A. Balows et al. (ed.), The prokaryotes. Springer, New York.

33. Woese, C. R., O. Kandler, and M. L. Wheelis. 1990. Toward a natural

system of organisms: proposal for the domains Archaea, Bacteria, and Eucarya. Proc. Natl. Acad. Sci. USA. 87: 4576-4579.

34. Yang, S. Y., and H. Schulz. 1983. The large subunit of the fatty acid oxidation complex from *Escherichia coli* is a multifunctional polypeptide. J. Biol. Chem. 258: 9780-9785.

Chapter 3

GENTISATE 1,2-DIOXYGENASE FROM *HALOFERAX* SP. D1227

Abstract

Gentisate 1,2-dioxygenase from extreme halophile *Haloferax* sp. D1227 was purified using a three-step procedure. The enzyme was found to be a homotetramer of 42,000±1,000 Da subunits with a native molecular weight of 174,000±6,000 Da. The optimal salt concentration, temperature and pH for enzyme activity were 2 M KCl or NaCl, 45°C and pH 7.2, respectively. The gene encoding *Hf.* D1227 gentisate 1,2-dioxygenase was cloned, sequenced and expressed in *Hf. Volcanii*. The deduced amino acid sequence exhibited a 9.2% excess acidic over basic amino acids typical of halophilic enzyme. Four noval histidine clusters and a possible extradiol dioxygenases fingerprint region were identified.

Introduction

Under aerobic conditions, aromatic compounds are transformed by monooxygenases and dioxygenases into dihydroxylated central intermediates including gentisate, catechol, and protochatechuate, which are subsequently cleaved by ring-fission dioxygenases (12). Intradiol dioxygenases such as catechol 1,2-dioxygenase and protocatechuate 3,4-dioxygenase cleave between the two hydroxyl groups (*ortho* cleavage) and typically contain nonheme Fe^{3+}, whereas extradiol dioxygenases such as catechol 2,3-dioxygenase and protocatechuate 4,5-dioxygenase cleave at a bond proximal to one of the two hydroxyl groups (*meta* cleavage) and contain Fe^{2+}. Phylogenetic analyses have indicated that while enzymes within each class are evolutionarily related, intradiol and extradiol dioxygenases have arisen from different ancestors (7, 13, 21). Gentisate 1,2-dioxygenase can't be classified as either intradiol or extradiol, since the cleavage of gentisate occurs between the carboxyl substituent and the proximal hydroxyl group. Gentisate 1,2-dioxygenases from *Moraxella osloensis*, *Pseudomonas testosteroni*, *Pseudomonas acidovorans*, *Bacillus stearothermophilus* PK1, and *Rhodococcus erythropolis* S-1, have been

purified and characterized (2, 14, 16, 24). The enzymes from *P. testosteroni* and *P. acidovorans* have been demonstrated to contain active site Fe^{2+} with coordination sites for both the substrate and O_2 suggesting that gentisate 1,2-dioxygenases in these organisms are mechanistically more similar to extradiol dioxygenases (14).

Haloferax sp. D1227, an extreme halophile isolated from soil contaminated with highly saline oil brine near Grand Rapids, Michigan, is the only reported aerobic archaeon utilizing aromatic compounds (i.e., benzoic acid, cinnamic acid, and 3-phenylpropionic acid) as sole carbon and energy sources for growth (8). During our study of the 3-phenylpropionic acid metabolism by *Hf.* D1227 (10), gentisate 1,2-dioxygenase activity was demonstrated in cell-free extracts prepared from cells grown on 3-phenylpropionic acid, cinnamic acid or benzoic acid. Examination of gentisate 1,2-dioxygenase from this extreme halophile was therefore undertaken. In this communication, we report the purification and characterization of gentisate 1,2-dioxygenase from *Hf.* D1227, as well as the cloning, sequencing and expression of the gene encoding *Hf.* D1227 gentisate 1,2-dioxygenase.

Materials and Methods

Materials. All chemicals used in this study were reagent grade. Benzoic acid and cetyltrimethylammonium bromide (CTAB) were purchased from Aldrich Chemical Co. (Milwaukee, WI.). Catechol, protocatechuic acid, gentisic acid, $Fe(NH_4)_2(SO_4)_2$, 2,2'-dipyridyl, ascorbic acid, SDS and PVDF membrane were obtained from Sigma chemical Co. (St. Louis, MO.). Phenyl-Sepharose CL-4B, Bio-Gel Hydroxyapatite and Superose^{TM}12 prepacked column were from Pharmacia Fine Chemicals (Uppsala, Sweden). N,N,N',N',-tetramethylethylenediamine (TEMED), acrylamide, bisacrylamide, ammonium persulfate, restriction enzymes and T4 DNA ligase were purchased from Boehringer Mannheim Corporation (Indianapolis, IN.). X-Gal, isopropylthio-β-D-galactoside (IPTG) and *Taq* DNA polymerase were obtained from Life Technologies (Grand Island, NY.). GENECLEAN II Kit was obtained from BIO 101 Inc.(La Jolla, CA.).

Microorganisms, plasmid vector, media, and growth conditions. *Haloferax* sp. D1227 has been described (8). *Haloferax volcanii* WFD11 was obtained from Dr. W. F. Doolittle (Dalhousie University, Halifax, Canada). pBluescript SK(+) was purchased from Strategene (La Jolla,

CA.). Plasmid vector pMDS30 was a gift from Dr. M. L. Dyall-Smith (University of Melbourne, Parkville, Australia).

For growth of *Hf.* D1227 on benzoic acid, BS3 mineral salts medium (8) of the following composition (in g/l) was used: $(NH_4)_2SO_4$, 0.33; KCl, 6.0; $MgCl_2 \cdot 6H_2O$, 12.1; $MgSO_4 \cdot 7H_2O$, 14.8; KH_2PO_4, 0.34; $CaCl_2 \cdot H_2O$, 0.36; and NaCl, 100. 1 ml/l of a trace element solution (25) was also added prior to sterilization, and the pH was adjusted to 6.9 with KOH. Filter-sterilized benzoic acid was added after sterilization. For rich medium (BSYT), BS3 mineral salts medium was supplemented with 3 g/l yeast extract and 3 g/l tryptone. *E. coli DH5α* was grown on LB medium (18). For solid media, 15 g/l Bacto-agar was added prior to autoclaving.

Cells were cultured aerobically in Erlenmeyer flasks containing 1/4 volume of medium. Flasks were incubated at 37°C on a rotary shaker at 200 rpm. Growth was monitored by measuring OD_{600nm} on a Gilford DU spectrophotometer.

Enzyme assay and protein determination. Unless stated otherwise, Gentisate 1,2-dioxygenase was assayed at room temperature by measuring the formation of maleylpyruvate at 334 nm for 30 seconds with a Perkin

Elmer double beam 124 spectrophotometer (17). The reaction mixture (2 ml) contained 0.25 mM gentisic acid, 50 µl enzyme, and 100 mM potassium phosphate buffer (pH 7.0) containing 2 M KCl. The reference cuvette contained the same reaction buffer except gentisic acid. One unit of enzyme activity was defined as the amount of enzyme that catalyzed the formation of 1 µmol maleylpyruvate/min. The molar absorption coefficient for maleylpyruvate (ε = 10,800) (2) was used to calculate enzyme activity.

Protein concentrations of the enzyme preparations were determined by the method of Bradford (1) with bovine serum albumin dissolved in 100 mM potassium phosphate buffer (pH 7.0) containing 2 M KCl as the standard.

Preparation of cell-free extracts. Mid-log phase cells grown on 3 mM benzoic acid were harvested by centrifugation at 10,600×*g* for 30 min. After washing twice with 1/5 culture volume of 100 mM potassium phosphate buffer (pH 7.0) containing 2 M KCl, cells were resuspended in 10 ml of the same buffer. 2.5 ml aliquots of the suspension were sonicated four times (30 seconds at 50 W followed by 2 min of cooling) in an ice bath using a 4710 Series Ultrasonic Homogenizer (Cole-Parmer Instrument Co.,

Chicago, IL.). After removing unbroken cells and cell debris by centrifugation at 47,800×*g* for 30 min (4°C), 5 mM ascorbic acid was added to the supernatant to stabilize the enzyme.

Enzyme purification. 10 ml cell-free extract was loaded onto a phenyl-Sepharose CL-4B column (6 cm×1.7 cm) equilibrated with 100 mM potassium phosphate buffer (pH 7.0) containing 2 M KCl and 5 mM ascorbic acid. The sample was eluted with the same buffer at a flow rate of 14 ml/hr. Fractions (0.55 ml) with high activity were pooled, diluted with equal volume of 10 mM potassium phosphate buffer (pH 7.0) containing 2 M KCl and 5 mM ascorbic acid, and loaded onto a hydroxyapatite column (3 cm×1.7 cm) equilibrated with the same buffer. The sample was eluted with 60 mM potassium phosphate buffer (pH 7.0) containing 2 M KCl and 5 mM ascorbic acid at a flow rate of 7 ml/hr. Fractions (0.55 ml) with high activity were pooled and concentrated to 200μl using a Centricon-10 concentrator (MW cut-off : 10,000. Amicon, Inc., Beverly, MA.). The concentrated sample was then loaded onto Superose^{TM}12 prepacked column (30 cm×1 cm) equilibrated with 100 mM potassium phosphate buffer (pH 7.0) containing 2 M KCl and 5 mM ascorbic acid and eluted with the same

buffer at a flow rate of 6 ml/hr. Fractions (0.55 ml) with the highest activity were pooled and stored at 4°C. All chromatographic steps were performed at 4°C except gel filtration which was carried out at room temperature on a Pharmacia FPLC system.

Estimation of native molecular mass and subunit molecular weight. The molecular weight of the native gentisate 1,2-dioxygenase was determined by gel filtration chromatography as described in the purification procedure. The column was calibrated with bovine thyroglobulin (M_r 669,000); horse spleen apoferritin (M_r 443,000); sweet potato β-amylase (M_r 200,000); yeast alcohol dehydrogenase (M_r 150,000); bovine serum albumin (M_r 66,000); and bovine erythrocytes carbonic anhydrase (M_r 29,000) in the MW-GF-1000 kit (Sigma).

The subunit molecular weight of gentisate 1,2-dioxygenase was obtained by CTAB-PAGE performed as described by Eley et al. (6). A 4% concentrating gel and a 12% separating gel were used. The samples were desalted by diafiltration with 100 mM potassium phosphate buffer (pH 7.0) using Centricon-10 prior to electrophoresis. Proteins were stained with Coomassie brilliant blue R-250 (11). Molecular weight standard SDS-6H

from Sigma was used. CTAB-PAGE was done at 30 mA and room temperature with cold water cooling of the buffer chamber.

N-terminal amino acid sequencing and peptide sequencing. The purified enzyme was run on SDS-PAGE and electroblotted onto PVDF membrane by the method of Matsudaira (19). The protein band stained with Coomassie brilliant blue R-250 was excised and submitted for N-terminal amino acid sequencing and peptide sequencing at MSU Macromolecular Structure Facility. For peptide sequencing, enzyme on the membrane was digested with trypsin at 37 °C for 20 hours and the peptides were separated by HPLC using a C_{18} column (0.8 mm × 250 mm) with a gradient of 5% acetonitrile to 50% acetonitrile. Both N-terminal amino acid sequencing and peptide sequencing were performed on a 494 Procise protein sequencer (Applied Biosystems, Weiterstadt, Germany) using automated Edman degradation.

Preparation of *Hf.* D1227 genomic DNA. Mid-log phase cells of *Hf.* D1227 grown in 100 ml BSYT medium were harvested by centrifugation at 10,600×*g* for 30 min. After washing twice with 100 mM potassium phosphate buffer (pH 7.0) containing 2 M KCl, the pellet was resuspended

in 50 ml distilled water for cell lysis. After removal of cell debris by centrifugation at 47,800×*g* for 30 min, the supernatant was extracted once with an equal volume of phenol, and twice with an equal volume of phenol/chloroform. DNA in the aqueous phase was precipitated with 2 volume of ethanol and 0.1 volume of 3 M sodium acetate (pH 5.2) at −16°C overnight. After centrifugation, the pellet was rinsed with 1 ml of 70% ethanol, air dried, and resuspended in 1 ml of H_2O. This preparation was then treated with RNase at a final concentration of 25 μg/ml.

Cloning and sequencing of *Hf.* D1227 gentisate 1,2-dioxygenase gene. A part of the open reading frame for the *Hf.* D1227 gentisate 1,2-dioxygenase gene was first obtained by PCR amplification of the *Hf.* D1227 genomic DNA using two degenerate primers derived from the purified *Hf.* D1227 gentisate 1,2-dioxygenase. The entire nucleotide sequence of the coding and flanking regions of the gene was then obtained by chromosomal walking using PCR techniques. The overall strategy for cloning the *Hf.* D1227 gentisate 1,2-dioxygenase gene is depicted in Figure 3.1. For this, a 226 bp fragment (segment a) of *Hf.* D1227 gentisate 1,2-dioxygenase gene was first obtained by PCR amplification of the *Hf.* D1227 genomic DNA

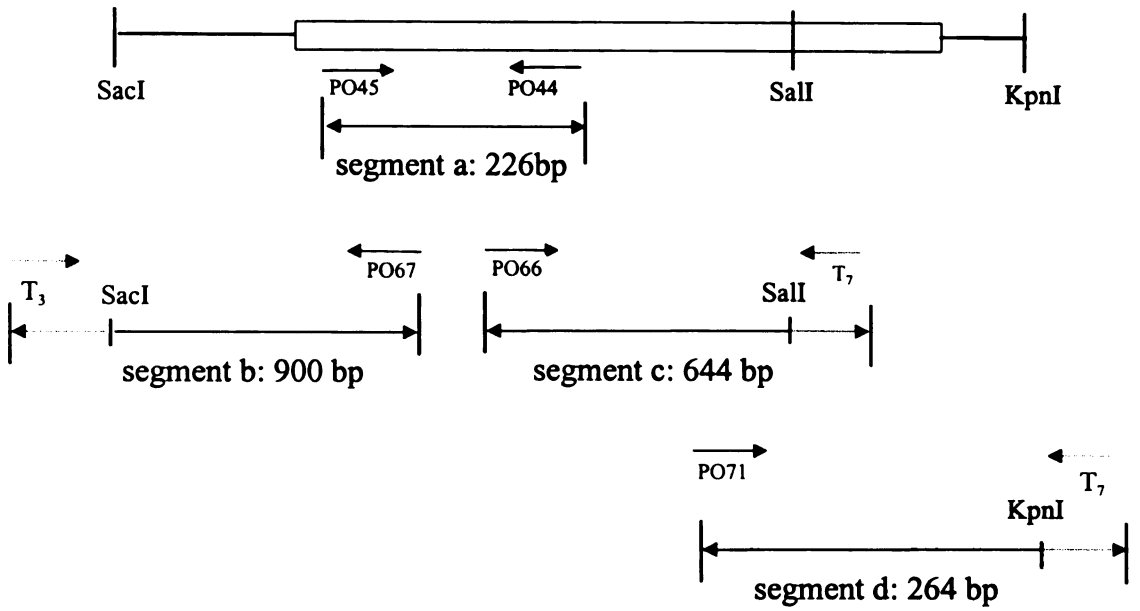

Figure 3.1 Strategy for cloning the coding and flanking regions of *Hf.* D1227gentisate 1,2-dioxygenase gene. The coding region is enclosed in the box. Solid lines represent *Hf.* D1227 sequences and dashed lines represent pBluescript SK(+) sequences

using forward primer PO45 [5'-GCIGA(A/G)CA(A/G)GA(A/G)CCIAA (A/G)GA-3'] and reverse primer PO44 [5'-TAICCIGT(A/G)TTIACIGG (A/T/C/G)AC-3'] corresponding to N-terminal sequences AEQEPKE and YGTNVPV from the intact enzyme and a tryptic peptide of the enzyme respectively. Segment a was sequenced using PO44 and PO45 as sequencing primers.

A 900 bp fragment (segment b) upstream and overlapping segment a was obtained by PCR amplification of the ligation mixture of *SacI*-digested genomic DNA and pBluescript SK(+) with primers T_3 from pBluescript SK(+) [5'-AATTAACCCTCACTAAAGGG-3'] and PO67 [5'-GCCGAA TTGGTT TCCGAAGT-3'] which is 88 bp downstream of the 5'end of segment a. Part of segment b was sequenced using PO67 as the sequencing primer. Segment c, a 644 bp fragment downstream and overlapping segment a, was obtained by PCR amplification of the ligation mixture of *SalI*-digested genomic DNA and pBluescript SK(+) with T_7 primer from pBluescript SK(+) [5'-GTAATACGACTCACTATAGG GC-3'] and PO66 [5'-TCTGGAAGTGGGAAGACATC-3'] which is 82 bp upstream of the 3'end of segment a. Segment c was sequenced using T_7 and PO66 as

sequencing primers. A 264 bp fragment (segment d) downstream and overlapping segment c was obtained by PCR amplification of the ligation mixture of *KpnI*-digested genomic DNA and pBluescript SK(+) with primers T_7 and PO71 [5'-TGTTTCCGACGATGTCGTTC-3'] which is 54 bp upstream of the 3'end of segment c. The sequence of segment d was determined using T_7 and PO71 as sequencing primers.

The PCR reaction mixtures in a total volume of 100 µl contained: 2 µl of DNA template (ca. 100 ng), 20 mM Tris-HCl (pH 8.4), 50 mM KCl, 1.5 mM $MgCl_2$, 0.25 mM of each dNTP, 2.5U of *Taq* DNA polymerase, and 30 pmol of each primer. PCR reactions were carried out on Perkin Elmer GeneAmp PCR System 2400 (Perkin Elmer, Norwalk, CT.) and thermal cycling conditions were 94°C for 5 min followed by 35 cycles of 94°C for 1 min, 55°C for 1 min, and 72°C for 3 min. A final extension was performed at 72°C for 6 min. PCR products were purified with GENECLEAN II Kit following the protocol recommended by the manufacturer. Nucleotide sequencing was done at the Nucleic Acid Sequencing Facility of Michigan State University with an ABI Prism sequencer (Applied Biosystems).

Expression of *Hf.* D1227 gentisate 1,2-dioxygenase gene in *Hf. volcanii* WFD 11. A 1353 bp fragment encoding gentisate 1,2-dioxygenase gene and its flanking regions was amplified from the genomic DNA of *Hf.* D1227 using PO92 [5'-GCGGAAAGCTTTGG GAGTAC-3'] and PO93 [5'-TAGGTACCTACCCGGCCTGG-3']. PO92 corresponds to nucleotides 10 to 29 of the sequence shown in Figure 3.4 (see below) except that a G at position 21 was changed to a T in order to introduce a *Hind III* restriction site. PO93 corresponds to nucleotides 1346 to 1363 of the sequence with two random nucleotides T and A added to the 5'end for effective digestion at the *KpnI* site. PCR reaction and product purification were carried out as described above.

After double digestion with *Hind III* and *KpnI*, this 1353 bp fragment was ligated to plasmid pMDS30 which had been cut with the same two enzymes. Transformation of the resulting plasmid into *E. coli DH5α* and the plasmid isolation from *E. coli* transformants were performed using standard methods (18). Transformation of the resulting plasmid into *Haloferax volcanii* WFD 11 was carried out using the PEG method described by Holmes et al. (15). Transformants were selected on rich BSYT plates supplemented with 15%

sucrose and 0.3% novobiocin. Confirmed to contain the 1353 bp insert by PCR amplification with PO92 and PO93, one colony was inoculated into 10 ml BS3 medium containing 5 mM pyruvate and 0.3% novobiocin, and the gentisate 1,2-dioxygenase activity was measured as described in **Enzyme assay**.

Results

Purification of gentisate 1,2-dioxygenase from *Haloferax* sp. D1227.

The soluble gentisate 1,2-dioxygenase from *Hf.* D1227 was purified 207-fold from cell-free extracts of benzoic acid-grown cells in three steps with 54% yield to give a preparation with a specific activity of 187 U/mg (Table 3.1). This preparation was electrophoretically homogeneous, showing one band on an CTAB-PAGE gel (Figure 3.2). All purification steps were performed in the presence of 2 M KCl, since *Hf.* D1227 gentisate 1,2-dioxygenase lost its activity irreversibly in low salt concentrations. Ascorbic acid, which proved to be an stabilizer for the enzyme, was added to all the purification buffers.

Table 3.1 Purification of gentisate 1,2-dioxygenase from *Hf.* D1227

Step	Total protein (mg)	Total activity (U)	Specific activity (U/mg)	Yield (%)	Purification (fold)
Crude extract	114	104	0.9	100	1
Phenyl Sepharose Cl-4B	19	100	5.3	96	6
Hydroxyapatite	1.7	84	49.4	80	55
Superose 12	0.3	56	186.7	54	207

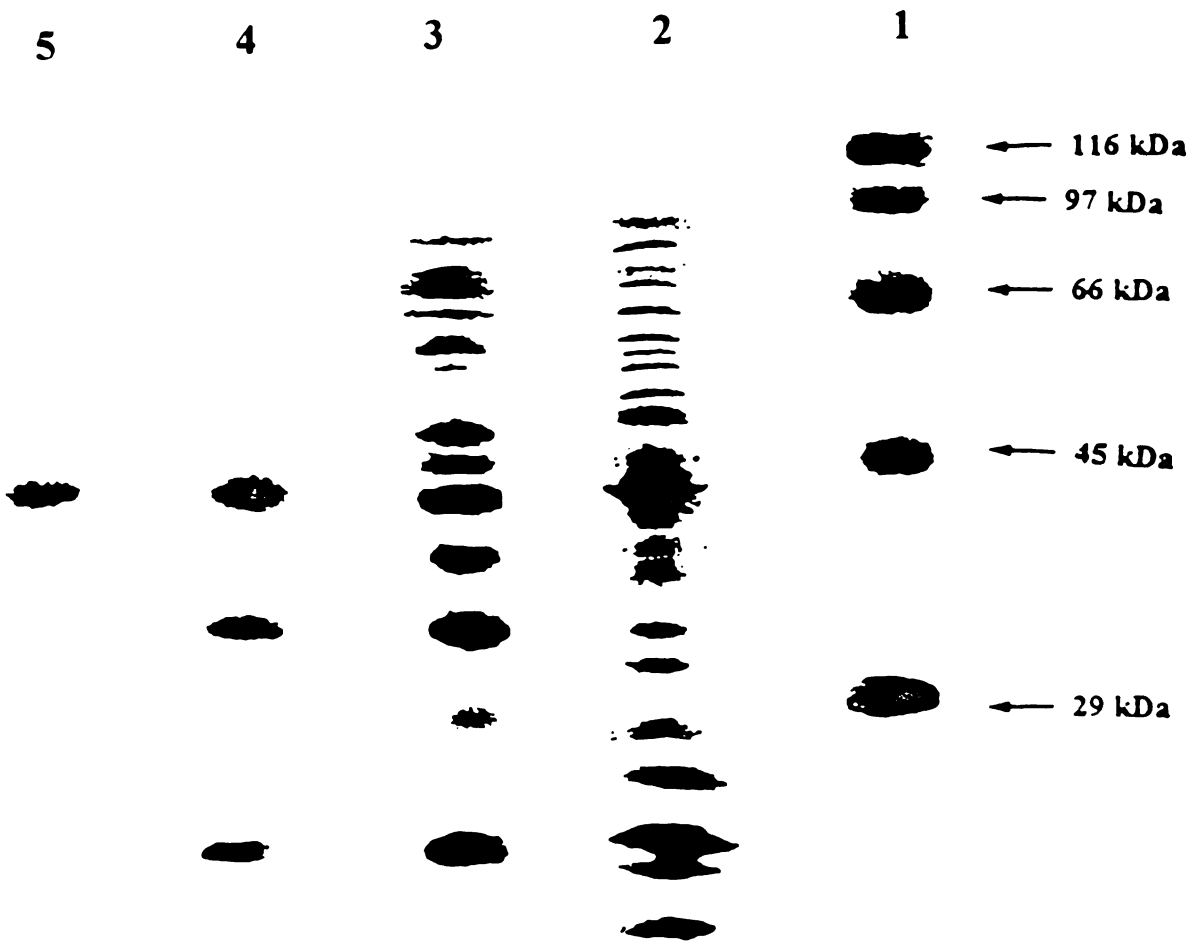

Figure 3.2 CTAB polyacrylamide electrophoresis of *Hf.* D1227 gentisate 1,2-dioxygenase at different stages of purification. 1. marker proteins; 2. crude extract; 3. phenyl Sepharose Cl-4B; 4. hydroxyapatite; 5. superose 12.

Molecular weight and subunit structure. The molecular weight of the native purified *Hf.* D1227 gentisate 1,2-dioxygenase was estimated to be 174,000±6,000 by gel filtration. The subunit molecular weight of the purified enzyme estimated by CTAB-PAGE was 42,000±1,000. These results suggest that *Hf.* D1227 gentisate 1,2-dioxygenase is a tetramer composed of four equally sized 42 kDa subunits. CTAB-PAGE instead of SDS-PAGE was used in subunit molecular weight estimation in this study because it has been demonstrated (20) that electrophoresis with this cationic detergent is a more accurate method to determine the subunit molecular weight of halophilic proteins, as halophilic proteins only bind a small amount of SDS, resulting in a reduced mobility and an overestimation of the molecular weight.

N-terminal amino acid sequencing and peptide sequencing. Amino acid residues at the N-terminus of *Hf.* D1227 gentisate 1,2-dioxygenase were determined to be A-E-Q-E-P-K-E-L-L-E-M-S-T-D-T-E-R-L-L-E-E-N-D-L-R-P-L-W-E-V-E-K-D-F-G-N-Q-F-G-G-. The N-terminal sequence of one tryptic peptide of this enzyme was also obtained: V-A-V-P-V-N-T-G-Y-R-. This peptide sequence along with N-terminal sequence were used in

gene cloning and sequencing (see below). Among the five purified gentisate 1,2-dioxygenases, only N-terminal sequences of *P. testosteroni* and *P. acidovorans* enzymes have been reported, and these have no sequence similarity with that of *Hf.* D1227 gentisate 1,2-dioxygenase.

Effect of salt, temperature and pH on the activity and stability of the purified *Hf.* D1227 gentisate 1,2-dioxygenase. The salt dependence of *Hf.* D1227 gentisate 1,2-dioxygenase activity is shown in Figure 3.3, exhibiting the highest activity in the presence of 2 M KCl. NaCl could substitute for KCl, yielding the same 2 M optimum. The optimal pH was pH 7.2 and the optimal temperature for the activity was 45°C (data not shown). The purified *Hf.* D1227 gentisate 1,2-dioxygenase lost activity rapidly and irreversibly in salt concentrations below 2 M KCl, with 40% of activity remaining when the enzyme was kept in 1.5 M KCl for 30 min in ice and assayed. This enzyme was also heat labile, incubation at 55°C for 10 min caused 96% loss of activity. The enzyme was stable over a narrow pH range (pH 6.5- 8.0). The enzyme in 100mM potassium phosphate buffer (pH 7.0) containing 2 M KCl was stable for up to three days at 4°C when 5 mM ascorbic acid or DTT was added.

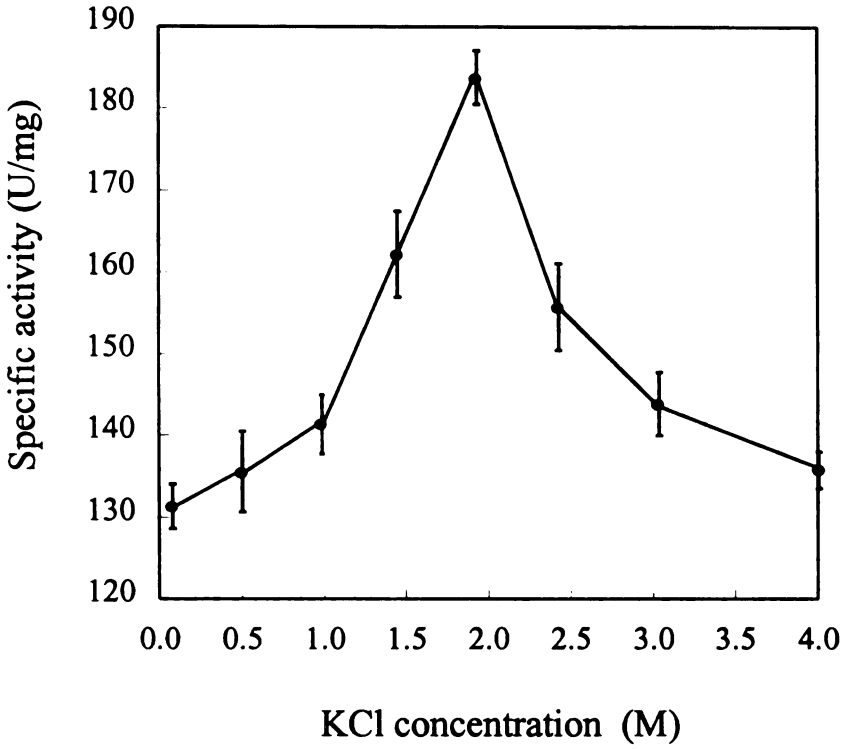

Figure 3.3 Effect of salt concentration on *Hf.* D1227 gentisate 1,2-dioxygenase activity

Catalytic properties and product identification. The V_{max} of the gentisate 1,2-dioxygenase reaction was 187 ± 24 U/mg and the K_m value for gentisic acid was 95 ± 8 μM. Flushing the reaction mixture with nitrogen gas caused 89% loss of enzyme activity, suggesting the involvement of O_2 in the reaction. Catechol and protecatechuate were not substrates for this enzyme. 2,2-dipyridyl was an inhibitor for the enzyme activity with an K_i value of 1.2 mM.

As a result of enzymatic gentisate oxidation, a compound with an absorbance maximum at 334 nm was observed, which was lost on acidification. These properties are characteristic of the expected maleylpyruvate product (17).

Cloning and sequencing of *Hf.* D1227 gentisate 1,2-dioxygenase gene. The gene encoding *Hf.* D1227 gentisate 1,2-dioxygenase was cloned and sequenced as described in **Materials and Methods.** The determined nucleotide sequence and the deduced amino acid sequence are shown in Figure 3.4. The open reading frame of this gene contains 1074 bp which encodes a protein of 358 amino acids with a molecular weight of 40,547. The deduced protein sequence of *Hf.* D1227 gentisate 1,2-dioxygenase had

```
   1 CCGAACTGGGCGGAAAGCTCTGGGAGTACGCCATTCAGGGGCAGATGGTCTGCGAGGAC
  61 GCCGCGAGCTGTACCCCTCGAAGGAGATATTCGACGCGCAGGTGAGCCAGTAGCGACCC
 121 GGTGGCGGGTGACGGGTGACGGTGTCCGCCCGTAGCGGCGCCACGCGACGAGAATAGAC
 181 CATACATTTATGAAGAATCCTCGGGAACTTTACACCATGGCTGAACAAGAGCCGAAGGA
                                          M  A  E  Q  E  P  K  E

 241 ACTCCTAGAGATGAGTACCGACACGGAGCGTCTCCTCGAGGAGAACGACCTGCGACCTCT
       L  L  E  M  S  T  D  T  E  R  L  L  E  E  N  D  L  R  P  L

 301 CTGGGAAGTCGAAAAGGACTTCGGAAACCAATTCGGCGGGTTCGAGGCGGACATCTGGAA
       W  E  V  E  K  D  F  G  N  Q  F  G  G  F  E  A  D  I  W  K

 361 GTGGGAAGACATCCAGGCGTCGATCGACGCCATCGAGCGGGACGTCCCCATCGCGGACCT
       W  E  D  I  Q  A  S  I  D  A  I  E  R  D  V  P  I  A  D  L

 421 CCCGCCGGGGTTCCAGCGACGCGTCGCCGTGCCCGTCAACACGGGATACCGAAACGCCAT
       P  P  G  F  Q  R  R  V  A  V  P  V  N  T  G  Y  R  N  A  I

 481 CTCGAACACGATTTACGTCGGCGTCCAGACCGTCTCGCCCGGCGAGACCGCGCCGGCACA
       S  N  T  I  Y  V  G  V  Q  T  V  S  P  G  E  T  A  P  A  H

 541 CCGACACGGGGCGAACGCGCTTCGGTTCACTATCGACGGGAGCGAGGACATGAAGACCGT
       R  H  G  A  N  A  L  R  F  T  I  D  G  S  E  D  M  K  T  V

 601 CGTCGCGGGCGAGGAGTTCCCGATGCGGGACAACGACCTCATCACGACGCCGCAGTGGGA
       V  A  G  E  E  F  P  M  R  D  N  D  L  I  T  T  P  Q  W  E

 661 GTGGCACGACCACGTCAACGACGGCGACGAGACGGCGGCGTGGCTCGACGTGCTCGACCT
       W  H  D  H  V  N  D  G  D  E  T  A  A  W  L  D  V  L  D  L

 721 CCCGCTCGTCCTCGACTCGCTCAACGCGCGCAACACCTTCGAGAACCACGAACTCGACCG
       P  L  V  L  D  S  L  N  A  R  N  T  F  E  N  H  E  L  D  R

 781 CCAGCCCGTGACGAAGTCGCAGGGCTACTGGGAGTCGCAGTACGGACGCGCCCGCCCGTT
       Q  P  V  T  K  S  Q  G  Y  W  E  S  Q  Y  G  R  A  R  P  F

 841 GAGGACACGAAGGAAGACGGGATTCCCGGACCCTTCGAGGGGAACTGCGCCGCGACGCC
       E  D  T  K  E  D  G  I  P  G  P  F  E  G  N  C  A  A  T  P

 901 GCCGTACCGATTCAGCTGGAAAGACACCCTCCAGACCCTCCGACAGCGAGCCGAAAACGA
       P  Y  R  F  S  W  K  D  T  L  Q  T  L  R  Q  R  A  E  N  D

 961 CGACCCGGACCCGCACGACGGCTACAGTCTCTCGTACGTCAACCCCGCGACCGGCCAGCC
       D  P  D  P  H  D  G  Y  S  L  S  Y  V  N  P  A  T  G  Q  P

1021 CCGCTGTTTCCGACGATGTCGTTCCGCGCGCAGTTGCTTCAAGAAGAGACCGACCCGCA
       P  L  F  P  T  M  S  F  R  A  Q  L  L  Q  E  E  T  D  P  H
```

1081CTTCCACAACGCCGTCGACGCGTACTTCGTCATCGAGGGCGAGGGCGCGACGCACGTCGG
F H N A V D A Y F V I E G E G A T H V G

1141CGACGACGTGCTCGAATGGAGCGAACGCGACATCTTCGTGATTCCGCCGGACGAGATTCA
D D V L E W S E R D I F V I P P D E I **H**

1201 CCACCACGACCCCGACGGCGAAGCGATTCTCCTCGGGATGACCGACCGCCCGGTGTTCGA
H H D P D G E A I L L G M T D R P V F E

1261GGCGTTCAACTTCTACGCCGAGGCCGAACCGTAGGCGCGCGGGGTCCAGTTCCGGACCAC
A F N F Y A E A E P *

1321 TCTGTTCGCGCCTCGGCGGATACCGCCAGGCCGGGTAGGTACC

Figure 3.4 Nucleotide sequence of *Hf.* D1227 gentisate 1,2-dioxygenase gene and the deduced amino acid sequence. Amino acid sequences determined by protein sequencing are underlined. A putative promoter sequence is boxed. The histidine clusters are in bold letters. The putative conserved residues are double-underlined

a 9.2% excess acidic over basic amino acids with an isoelectric point of 4.15. A putative promoter sequence TTAT similar to the archaeal box A consensus TTA(T/A) usually located 27±4 bp upstream ATG start codon (4), was observed 25 bp upstream from the ATG translation initiation codon. Four histidine clusters H-X-H were found in the sequence, whose function is unclear, although it has been shown that histidine residues are involved in both iron ligand binding and catalytic function in eubacterial extradiol dioxygenases (7). When compared with sequences of ring-cleavage dioxygenases, a segment of *Hf.* D1227 gentisate 1,2-dioxygenase sequence encoding three residues (His, Tyr and Glu) conserved in the eubacterial extradiol dioxygenase fingerprint region (7) was identified (Figure 3.4).

Expression of *Hf.* D1227 gentisate 1,2-dioxygenase gene in *Hf. volcanii* WFD 11. The gentisate 1,2-dioxygenase activity of the *Hf. volcanii* transformant was 4.8±0.5U/g protein, which was 0.54% of the activity in *Hf.* D1227. No activity was detected in *Hf. volcanii* containing only shuttle vector pMSD30 without insert, and no increase of enzyme activity was detected when 0.5 mM benzoic acid was added as an inducer to

the growth medium.

Discussion

Gentisate 1,2-dioxygenase from *Hf.* D1227 is similar in molecular weight and subunit structure to those from *P. testosteroni*, *P. acidovorans*, and *M. osloensis* (2, 14), all being tetramers composed of four equal-sized subunits of molecular weight around 40 kDa. The gentisate 1,2-dioxygenase from *Bacillus stearothermophilus* is a homohexamer with a subunit molecular weight of 40 kDa and that of *Rhodococcus* is a homooctamer with a subunit molecular weight of 43 kDa (16, 24). Gentisate 1,2-dioxygenase from *Hf.* D1227 demonstrates a similar K_m value for gentisate with those of the two *Pseudomonas* enzymes and has a similar pH optimum (around pH 7.0) to four of the purified eubacteria enzymes. The exception is the *Rhodococcus* enzyme, exhibiting the maximal activity at pH 8.5.

Hf. D1227 gentisate 1,2-dioxygenase differs from the eubacterial counterparts in the requirement of 2 M KCl or NaCl for enzyme activity and stability. By possessing additional acidic residues (glutamic acid and aspartic acid), halophilic proteins are highly adapted to function in a high

salt milieu (3, 5, 9). Compared to the chemical neutrality of bulk protein for non-halophiles (23), *Hf.* D1227 gentisate 1,2-dioxygenase contains a 9.2% excess acidic over basic amino acids, which is typical of halophilic proteins (22, 23). The acidic amino acid content of the non-halophilic gentisate 1,2-dioxygenases has not been determined.

Four of the purified eubacteria gentisate 1,2-dioxygenases required exogenously added Fe^{2+} for enzyme activity. Although the gentisate 1,2-dioxygenase from *Hf.* D1227 did not require added Fe^{2+} for activity, $Fe(NH_4)_2(SO_4)_2$ could partially restore the lost activity of older *Hf.* D1227 enzyme preparations and 2,2'-dipyridyl was an inhibitor for this enzyme (10), suggesting the presence of Fe^{2+} in the enzyme.

Sequence comparison by BLAST showed no GenBank sequence similar to the *Hf.* D1227 gentisate 1,2-dioxygenase gene. This is not surprising given this enzyme's archaeal origin and the absence of eubacterial gentisate 1,2-dioxygenase sequences in the database. Although the expression of gentisate 1,2-dioxygenase in *Hf. volcanii* verified the function of the cloned gene, the expression level was quite low. Several factors might contribute to this low activity. First, the pMDS30 vector used does not have a

promoter adjacent to the *Hf.* D1227 gentisate 1,2-dioxygenase gene insert, and the control elements associated with the gentisate pathway were apparently not included with the cloned gene since induction of expression by benzoate was not observed. Secondly, the stability of the gentisate 1,2-dioxygenase and its mRNA in *Hf. volcanii* transformants is unknown.

In summary, gentisate 1,2-dioxygenase from extreme halophile *Haloferax* sp. D1227 is similar to its eubacterial counterparts in terms of subunit size and metal participation. The enzyme also possesses the properties characteristic of halophilic enzymes including the requirement of 2 M KCl or NaCl for activity and stability, and an excess of acidic over basic amino acids. It will be of interest to determine whether the four histidine clusters in the *Hf.* D1227 gentisate 1,2-dioxygenase gene are features shared by eubacterial gentisate 1,2-dioxygenases. Although a segment of the *Hf.* D1227 gentisate 1,2-dioxygenase contains the histidine, tyrosine and glutamic acid residues conserved in the eubacterial extradiol dioxygenase fingerprint region, further genetic and structural studies will be required to confirm that these residues are involved in metal binding and active site function of the dioxygenase.

Acknowledgments

We wish to thank Michael L. Dyall-Smith for plasmid vectors and assistance. We are extremely grateful to Robert Hausinger for help with purification. We also thank Olga Maltseva and Tae-Kyou Cheong for many helpful discussions. This work was partially supported by the MSU Biotechnology Research Center.

References

1. Bradford, M. M. 1976. A rapid and sensitive method for the quantitation of microgram quantities of protein utilizing the principle of protein-dye binding. Anal. Biochem. 72: 248-254.

2. Crawford, R. L., S. W. Hutton, and P. J. Chapman. 1975. Purification and properties of gentisate 1,2-dioxygenase from *Moraxella osloensis*. J. Bacteriol. 121: 794-799.

3. Dennis, P. P., and L. C. Shimmin. 1997. Evolutionary divergence and salinity-mediated selection in halophilic archaea. Microbiol. Mol. Biol. Rev. 61: 90-104.

4. Dennis, P. P. 1993. The molecular biology of halophilic archaebacteria. 274-279. In: R. H. Vreeland et al. (ed.), The biology of halophilic bacteria. CRC Press, Inc., Florida.

5. Dym, O., M. Mevarech, and J. L. Sussman. 1995. Structural features that stabilize halophilic malate dehydrogenase from an archaebacterium. Science. 267: 1344-1346.

6. Eley, M. H., P. C. Burns, C. C. Kannapell, and P. S. Campbell. 1979. Cetyltrimethylammonium bromide polyacrylamide gel electrophoresis: estimation of protein subunit molecular weights using cationic detergents. Anal. Biochem. 92: 411-419.

7. Eltis, L. D., and J. T. Bolin. 1996. Evolutionary relationships among extradiol dioxygenases. J. Bacteriol. 178: 5930-5937.

8. Emerson, D., S. Chauhan, P. Oriel, and J. A. Breznak. 1994. *Haloferax* sp. D1227, a halophilic Archaeon capable of growth on aromatic compounds. Arch. Microbiol. 161: 445-452.

9. Frolow, F., M. Harel, J. L. Sussman, M. Mevarech, and M. Shoham. 1996. Insights into protein adaptation to a saturated salt environment from the crystal structure of a halophilic 2Fe-2S ferredoxin. Nat. Struct. Biol. 3: 452-458.

10. Fu, W., and P. Oriel. 1997. Degradation of 3-phenylpropionic acid by *Haloferax* sp. D1227. Submitted.

11. Garfin, D. E. 1990. One-dimensional gel electrophoresis. 182: 425-441. In: Methods in enzymology. Academic Press, Inc., New York.

12. Gibson, D. T. and V. Subramanian. 1984. Microbial degradation of aromatic hydrocarbons. 181-252. In: D. T. Gibson (ed.), Microbial degradation of organic compounds. Marcel Dekker Inc., New York.

13. Harayama, S., M. Kok, and E. L. Neidle. 1992. Functional and evolutionary relationships among diverse dioxygenases. Annu. Rev. Microbiol. 46: 565-601.

14. Harpel, M. R., and J. D. Lipscomb. 1990. Gentisate 1,2-dioxygenase from *Pseudomonas*: purification, characterization and comparison of the enzymes from *Pseudomonas testosteroni* and *Pseudomonas acidovorans*. J. Biol. Chem. 265: 6301-6311.

15. Holmes, M. L., and M. L. Dyall-Smith. 1990. A plasmid vector with a selectable marker for halophilic archaebacteria. J. Bacteriol. 172: 756-761.

16. Kiemer, P., B. Tshisuaka, S. Fetzer, and F. Lingens. 1996. Degradation of benzoate via benzoyl-coenzyme A and gentisate by *Bacillus stearothermophilus* PK1, and purification of gentisate 1,2-dioxygenase. Biol. Fertil. Soils. 23: 307-313.

17. Lack, L. 1959. The enzymic oxidation of gentisic acid. Biochem. Biophys. Acta. 34: 117-123.

18. Maniatis, T., E. F. Fritsch, and J. Sambrook. 1982. Molecular cloning: a laboratory manual. Cold Spring Harbor Laboratory Press, Cold Spring Harbor, New York.

19. Matsudaira, P. 1987. Sequence from picomole quantities of proteins electroblotted onto polyvinylidene difluoride membranes. J. Biol. Chem. 262 :10035-10038.

20. Monstadt, G., and A. W. Holldorf. 1990. Arginine deminase from *Halobacterium salinarium*: purification and properties. Biochem. J. 273: 739-745.

21. Neidle, E. L., C. Hartnett, S. Bonitz, and L. N. Ornston. 1988. DNA sequence of the *Acinetobacter calcoaceticus* catechol 1,2-dioxygenase I structural gene *cat*A: evidence for evolutionary divergence of intradiol dioxygenases by acquisition of DNA sequence repetitions. J. Bacteriol. 170: 4874-4880.

22. Prub, B., H. E. Meyer, and A. W. Holldorf. 1993. Characterization of the glyceraldehyde 3-phosphate dehydrogenase from the extremely halophilic archaebacterium *Haloarcula vallismortis*. Arch. Microbiol. 160: 5-11.

23. Reistad, R. 1970. On the composition and nature of the bulk protein of the extremely halophilic bacteria. Arch. Microbiol. 71: 353-360.

24. Suemori, A., R. Kurane, and N. Tomizuka. 1993. Purification and properties of gentisate 1,2-dioxygenase from *Rhodococcus erythropolis* S-1. Biosci. Biotechnol. Biochem. 57: 1781-1783.

25. Widdel, F., and F. Bak. 1992. Gram-negative mesophilic sulfate-reducing bacteria. 3342-3378. In: A. Balows et al. (ed.), The prokaryotes. Springer, New York.

Chapter 4

SUMMARY AND RECOMMENDATIONS FOR FUTURE RESEARCH

Summary of the dissertation research findings

The first aromatic degradation pathway in Archaea is elucidated in this study. *Haloferax* sp. D1227 metabolizes 3-phenylpropionic acid by 2-carbon scission of the aliphatic side chain via a β-oxidation mechanism to produce benzoylCoA, which is further degraded via a gentisate pathway. The upper aliphatic pathway from 3-phenylpropionic acid to benzoic acid is separately regulated from the lower aromatic gentisate pathway. Although it has been proposed by Webley et al. (2) that *Nocardia opoca* metabolizes 3-phenylpropionic acid to benzoate via a mechanism similar to fatty acid β-oxidation based on their observation of the transient accumulation of cinnamic acid and benzoic acid in the 3-phenylpropionic acid-grown cultures, our study is the first to demonstrate the enzymes involved in the pathway.

The purified *Hf.* D1227 gentisate 1,2-dioxygenase involved in the 3-phenylpropionic acid degradation is similar to its eubacterial counterparts in terms of subunit size and metal participation. The enzyme also has properties characteristic of halophilic enzymes including the requirement of 2 M KCl or NaCl for activity and stability, and an excess of acidic over basic amino acids. The gene encoding *Hf.* D1227 gentisate 1,2-dioxygenase was cloned, sequenced and expressed in *Hf. volcanii.* The gene contains a sequence resembling the extradiol dioxygenases fingerprint region and four histidine clusters (H-X-H) whose function and distribution among eubacteria gentisate 1,2-dioxygenases remain unknown.

Future research

One area of future research could be to increase the expression level of *Hf.* D1227 gentisate 1,2-dioxygenase gene in *Hf. volcanni.* pMDS30 used in this study does not have a vector promoter adjacent to the *Hf.* D1227 gentisate 1,2-dioxygenase gene insert, so the endogenous promoter of the gene was used in the expression. It may be feasible to use those archaeal expression vectors containing promoters next to the polylinker regions, such as pWL107, pWL106, and pWL105 (1) to increase the expression.

Another area of research interest is the possible roles of the histidine clusters and the conserved histidine, tyrosine and glutamic acid residues in metal binding and active site function of *Hf.* D1227 gentisate 1,2-dioxygenase, for which site-directed mutagenesis should be performed. When the gene sequences of eubacteria gentisate 1,2-dioxygenases become available, they should be compared with our *Hf.* D1227 sequence.

The gentisate 1,2-dioxygenase activity was induced by benzoate in *Hf.* D1227, however, no benzoate induction was demonstrated in *Hf. volcanii* transformants, indicating control elements were not complete in the cloned gene. So, sequences adjacent to the cloned gene should be determined to detect the possible open reading frames and regulatory elements. This may also uncover the benzoate and 3-hydroxybenzoate hydroxylase activities possibly involved in 3-phenylpropionic acid degradation by *Hf.* D1227.

It will also be of interest to study the enzymes involved in the upper aliphatic pathway of 3-phenylpropionic acid degradation by *Hf.* D1227 and their relationships with fatty acid β-oxidation enzymes.

Reference

1. Lam, W. 1989. Unpublished data.

2. Webley, D. M., R. B. Duff, and V. C. Farmer. 1955. Beta-oxidation of fatty acids by *Nocardia opaca.* J. Gen. Microbial. 13: 361-369.

APPENDIX

APPENDIX

Degradation of Pinene by *Bacillus pallidus* BR 425

Abstract

An aerobic thermophile has been isolated from an α- and β-pinene enrichment culture possessing the ability to grow on the monoterpenes α- and β-pinene, pinocarveol, limonene, carveol, and carvone as sole carbon sources. The isolate which was designated BR425 has been tentatively identified as *Bacillus pallidus* using 16S ribosomal RNA gene sequencing and organism morphology. Biphasic incubations of BR425 cells with α-pinene, β-pinene, and limonene yielded carveol as a common metabolite, and an unusual enzyme activity in BR425 crude extracts catalyzing conversion of pinene to carveol utilizing FAD and potassium ferricyanide as electron acceptors was observed.

Introduction

Pinene, the major constituents of turpentine, are bicyclic monoterpenes which are produced in significant quantities by plants of the *Pinaceae*

family. Because of their volatility, pinene emission from conifer forests and during pulping operations constitute a major source of biogenic hydrocarbons (11, 17). The metabolism of pinene by microorganisms has been little studied, as they have limited water solubility, and are membrane-destructive to procaryotic and eucaryotic microorganisms (1). In early reports in which a number of pinene metabolites were identified, catabolism of α-pinene by *Pseudomonas* strain PL was suggested to proceed by isomerization of the pinene to limonene with subsequent oxidation to perillic acid prior to ring cleavage and further catabolism utilizing a β-oxidation pathway (16). An alternative pathway through limonene proposed by Gibbon and Pirt (7) has been questioned (18). A third pathway and some of the participating enzymes for *Nocardia* strain P18.3 (8) and *Pseudomonas fluorescens* strain NCIMB 11671 (2) have been described, in which α-pinene is directly oxidized to pinene epoxide prior to ring cleavage. Recent evidence indicates the presence of an alternative pinene pathway in the pinene-epoxidizing *Pseudomonas fluorescens* strain NCIMB 11671, the metabolites for which have not yet been identified (5). Few of the enzymes participating in pinene catabolism or their encoding genes have so far been characterized.

Because of their important environmental roles including composting and waste treatment at elevated temperature, our laboratory has been engaged in exploring the metabolic diversity of aerobic thermophilic bacteria. In this report, we provide initial information on the degradation of α- and β-pinene by a newly isolated *Bacillus* thermophile, which has been tentatively identified as a strain of *B. Pallidus*.

Materials and Methods

Reagents and Media. The (R)-enantiomer of α-pinene was selected for microbial degradation studies as this isomer predominates in North America pines. All monoterpenes were purchased from Aldrich Company (Milwaukee, Wisconsin), examined for purity using GC/MS (see below), and filter sterilized prior to use. M9 minimal salts medium (13) contained (per liter) Na_2PO_4, 6g; KH_2PO_4, 3g; NaCl, 0.5g; NH_4Cl, 1g; pH 7.4. After autoclaving and cooling, 2 ml of 1M $MgSO_4$ were added. LB medium has been described (13).

Organism isolation and growth. Pinene-degrading thermophiles were isolated from samples of dried wound exudate from a stand of white pine tree near Midland, Michigan. Enrichments were carried out in a 125 ml

bottle containing 50 ml M9 minimal salts and 0.05 ml α-pinene, and were incubated at 60 °C in a gyrorotatory water bath shake. After 72 hours incubation, samples of the enrichment culture were diluted and grown at 60 °C on M9 salt plates in Petri dishes containing α-pinene in small glass tubes attached to the cover. Isolates were repeatedly transferred on these plates and retained as putative pinene utilizers. One isolate, designated BR425, exhibited vigorous α-pinene-dependent growth, and was chosen for further study.

For examination of growth rates and metabolite production, isolate BR425 was grown in 100 ml serum bottles containing 49 ml M9 salts and pinene at the desired concentration and sealed with Teflon-coated stoppers and aluminum caps. Bottles were incubated in a gyrorotatory water bath shake. Colony-forming units were enumerated by plating on LB agar at 60 °C.

Extraction and analysis of pinene biotransformation products. For analysis of pinene biotransformation products, liquid cultures of BR425 grown for the desired time were centrifuged at 12,000×*g* for 20 minutes at 4 °C, acidified to pH 2.0 with HCl and extracted three times with equal volumes of ether. The ether fraction was evaporated to 25 ml and separated into neutral and acidic fractions by extraction (3 × 0.6 volumes) with 5%

NaOH. The ether fraction was concentrated with nitrogen, neutralized with 5% HCl, and analyzed by GC/MS. The NaOH fraction was acidified to pH 2.0 and reextracted (3 × 0.3 volumes) with ether. Following concentration, the ether fraction was analyzed using a Hewlett-Packard HP 5890 gas chromatograph with a MSDHP 5970 detector and a fused silica capillary column (0.25mmI.D. × 30M DB-wax). Conditions used were: helium carrier gas, injection port and detector port at 240 °C, column temperature from 40-240 °C at 7 °C/min with 2 min initial hold time.

Two-phase biotransformation studies. For two-phase biotransformation studies by suspensions of pinene-grown BR425 cells, 50 ml of BR425 cells grown in LB medium were washed with M9 medium and resuspended to 10^9 cells per ml in 0.05 M K_2HPO_4 buffer, pH 7.0 with 0.6 ml of pinene or limonene added. Following shaking in a gyrorotatory water bath at 50 °C, samples of the monoterpene phase were injected into the GC/MS for directe analysis.

16S ribosomal RNA sequence analysis. Partial analysis of the BR425 16S ribosomal RNA gene sequence was obtained using chromosomal DNA prepared as described by Maniatis et al. (8). PCR amplification and sequencing of the 16S ribosomal gene was carried out as described by

Maltseva et al. (12) using the Michigan State University Automated Sequencing Facility. Sequences were analyzed using the ribosomal database accessed using the GCG program (Genetics Computer Group, Madison, WI).

Assay of pinene oxide lyase. For assay of pinene oxide lyase, cells grown in LB broth into late exponential phase were disrupted using brief bursts of sonification at 4 °C followed by removal of cell debris by centrifugation for 30 minutes at 12,000×*g*. Enzyme assay utilized the spectrophotometric procedure of Griffiths et al. (8).

Pinene hydroxylase measurement in crude extracts. Pinene hydroxylase activity in crude extracts was measured utilizing BR425 cells grown in M9 salts containing 0.1% glycerol and 0.2% α-pinene at 50 °C to late exponential phase. Cells were centrifuged and resuspended in 5 ml 0.05M Tris buffer, pH 8.0 to which 5 µl phenylmethylsulfonylfloride added to inhibit proteases. Cells were sonicated using a Cole-Parmer 4710 ultrasonic homogenizer for 3 minutes in 30 second bursts with cooling, and centrifuged at 12,000×*g* for 30 minutes to provide a crude enzyme extract. Pinene hydroxylase was assayed in a mixture to which 200 µl crude enzyme was added to 800 µl containing 50 mM α-pinene, 1 mM FAD, 1 mM

potassium ferricyanide in 50 mM Tris buffer, pH 8.0. Carveol production was routinely measured with HPLC using 60% acetonitrile and 40% water eluant and a 3.9 ×150mm Nova-Pak C18 column (Waters). For enzyme assay under anoxic conditions, the crude enzyme extract and enzyme cocktail were separately sparged with nitrogen gas for 20 minutes prior to mixing and assay. For GC/MS analysis of enzyme reaction products, the filtered enzyme reaction mixture was extracted three times with ether and analyzed following ether evaporation using nitrogen gas.

Results

Characterization of isolate BR425. Isolate BR425 was plated from an α-pinene enrichment culture of white pine sap exudate and demonstrated good growth on M9 plates with either α- or β-pinene vapor, producing small creamy colonies in two days. Although the isolate exhibited a growth optimum at 55 °C (data not shown), a slower growth temperature of 50 °C was utilized for convenience. Microscopic examination indicated large rod-shaped bacteria with terminal endospores. Analysis of the 16S ribosomal gene sequence data approximately 350 nucleotides from each end yielded *Bacillus pallidus* (emb/z26930/BP16SRNA) as the best sequence match,

with the only sequence differences being G for A at position 6 and T for C at positon 573.

Growth of BR425 on monoterpenes. In previous studies with thermophile isolates growing on the monoterpene limonene, we found a limited concentraton range in which grouth was not inhibited (3). For isolate BR425 growing on α-pinene, a similar limited range was observed (Figure A1), with growth inhibition occurring above 0.2% concentration. The BR425 isolate was also shown to grow on a wide range but not all monoterpenes tested as shown in Table A1.

Metabolites produced during growth on α-pinene. Ether extracts of BR425 culture supernatants grown on α-pinene were examined at various times of culture with the results shown in Table A2. Significant amounts of the neutral metabolites pinocarveol, pinocarvone, carveol and carvone were observed together with lesser amounts of myrtenol, myrtenal, limonene, and β-pinene in two independent experiments. None of these metabolites were observed in the absence of the thermophile. For most metabolites, the highest concentrations were observed in the late exponential phase. In addition to these neutral metabolites, an acid metabolite of molecular mass 168 was observed showing the fragmentation pattern shown in Figure A2.

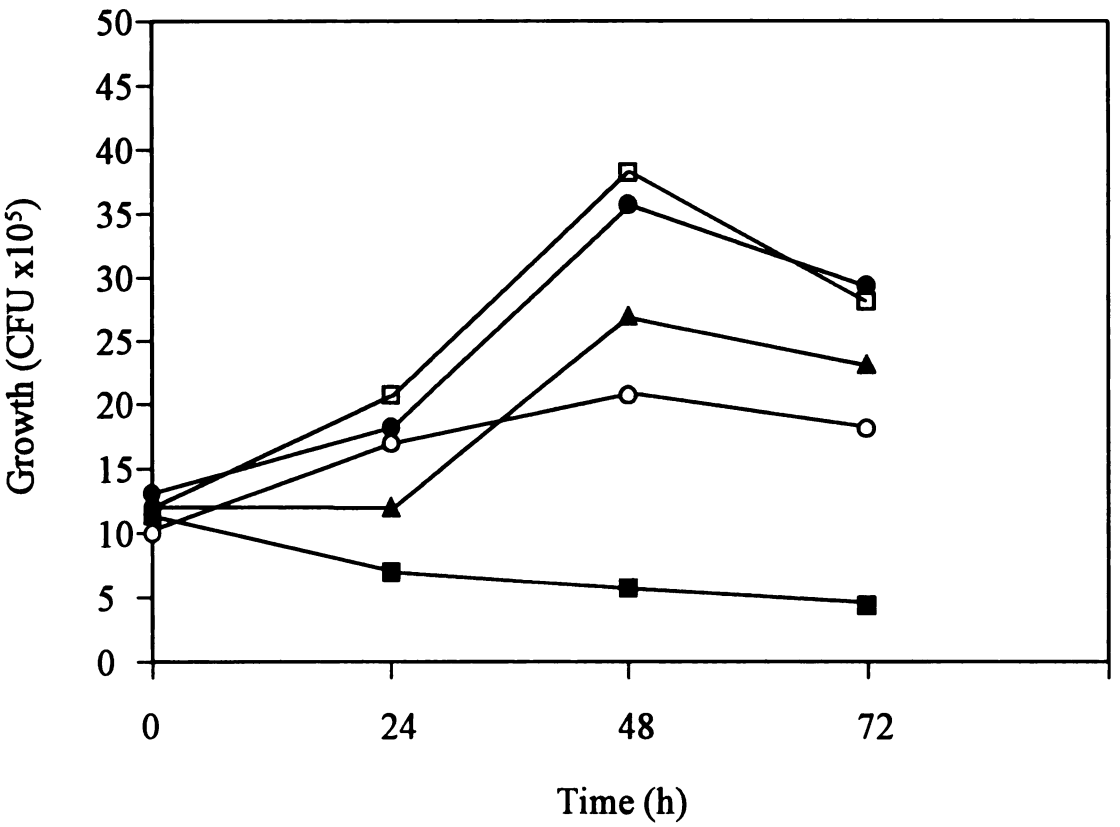

Figure A1 Growth of *Bacillus pallidus* BR425 in varied concentrations of (R)-α-pinene. ■, no pinene; ▲, 0.05% pinene; ●, 0.1% pinene, □, 0.2% pinene; ○, 0.3% pinene

Table A1 Growth of *B. pallidus* on monoterpenes

Monoterpenes	Optimal growth concentration
(R)-α-pinene	0.2%
(R)-Limonene	0.2%
(S)-α-pinene	0.1%
(S)-β-pinene	0.1%
(S)-carveol	0.1%
(S)-pinocarveol	0.05%
(S)-carvone	0.01%
Myrtenol, myrtenal, α-terpineol pinene epoxide	No growth

Table A2 Metabolites formed during growth of *B. pallidus* BR425 on α-pinene

Metabolites (mg/l)	0 hr	24 hr	48 hr	72 hr
β-pinene	0	0.01	0.03	0.02
Limonene	0	0.08	0.18	0.06
Pinocarveol	0	1.02	0.82	0.52
Pinocarvone	0	0.87	0.94	0.82
Myrtenol	0	0.58	0.52	0.32
Myrtenal	0	0.46	0.47	0.44
Carveol	0	4.38	6.32	1.48
Carvone	0	1.28	2.69	0.81

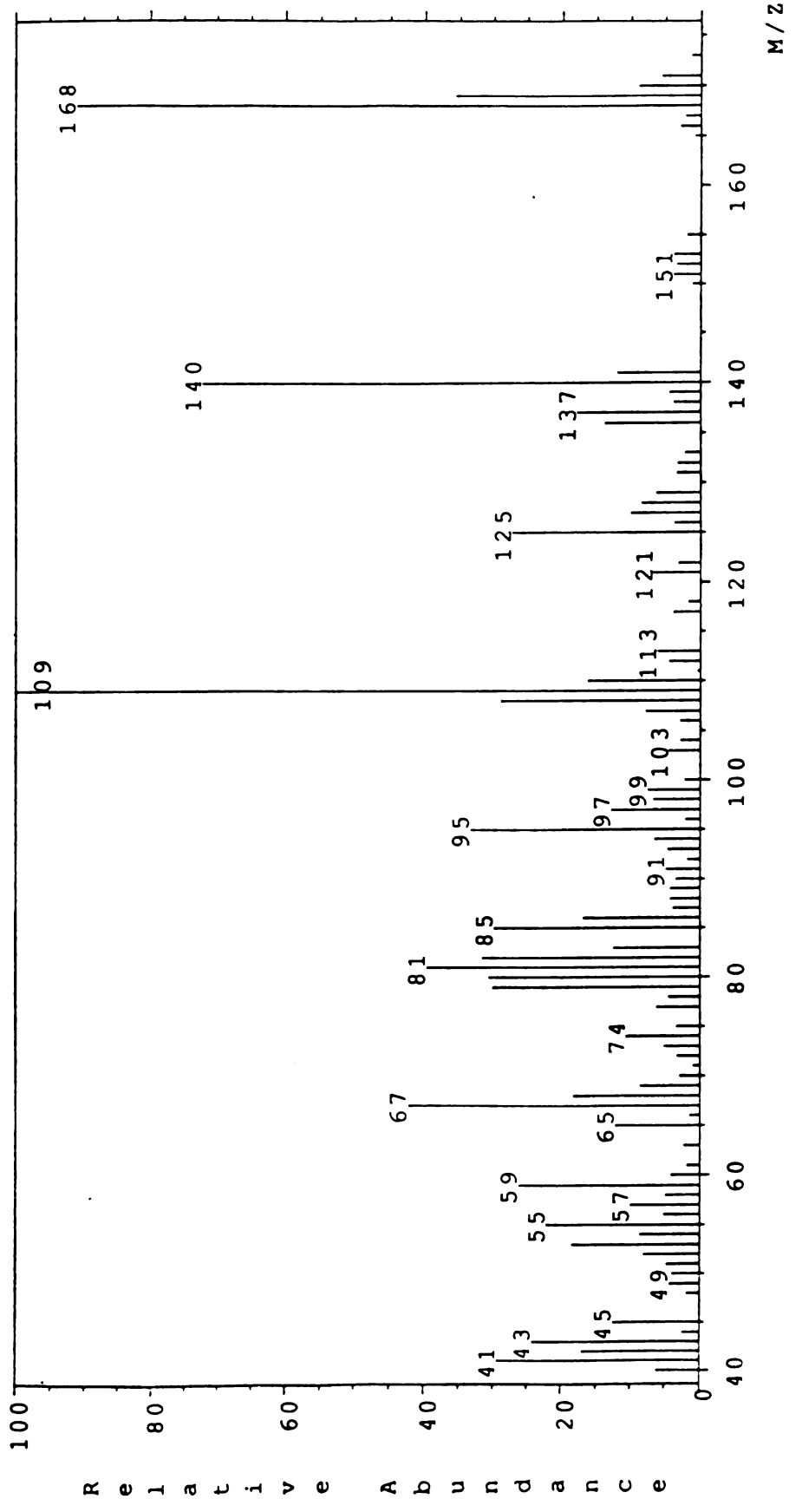

Figure A2 Fragmentation pattern of acid metabolite from BR425 growth on α-pinene or carvone

This acid metabolite was also observed during growth in carvone, and was not identified in a library search. This fragmentation pattern is similar but not identical with acid metabolites of the same mass number previously reported during growth of *Pseudomonas* strains on pinene (8, 19).

Metabolites produced during two-phase incubations with α-pinene and limonene. In previous work with a limonene-degrading *E. coli* recombinant (14), incubations with neat limonene provided a convenient method for identification of neutral terpenoid metabolites, as the organic phase insures saturation of substrate in the aqueous phase, while facilitating removal and concentration of metabolites in the organic phase which can be utilized for direct identification using GC/MS eliminating the need for aqueous extraction. Experiments using incubations using BR425 cell suspensions with α-pinene, β-pinene, and limonene are shown in Table A3. For incubations with α-pinene and β-pinene, similar metabolites were identified to those obtained by ether extraction during growth on α-pinene, except that metabolites were found in higher concentrations, and carvone was only observed in trace quantities. With limonene as substrate, carveol and carvone were found in significant quantities, together with a smaller amount of α-terpineol.

Table A3 Metabolites formed during two-phase incubation of BR425 suspended cells

Metabolites (mg/l)	Organic Phase		
	α-pinene	β-pinene	limonene
α-pinene		ND	ND
β-pinene	4.38		ND
Limonene	1.31	1.1	
Pinocarveol	20.5	19.3	ND
Pinocarvone	7.2	6.8	ND
Myrtenol	23.4	17.1	ND
Myrtenal	19.5	12.5	ND
α-terpineol	ND	ND	1.4
Carveol	14.3	9.6	10.2
Carvone	trace	trace	7.5

ND: not detected

α-pinene hydroxylase activity. In experiments with a cloned limonene degradation pathway in our laboratory, we have discovered a limonene hydroxylase with novel gene sequence whose action is unusual in utilizing the electron acceptor FAD and whose catalysis is not inhibited under anoxic conditions. A preliminary search for a similar hydroxylating activity for pinene in BR425 extracts indicated a α-pinene hydroxylase activity with added FAD and/or potassium ferricyanide shown in Table A4. Under anoxic conditions produced with nitrogen sparging of enzyme and reaction mixture prior to reaction, no inhibition of activity was observed. Although other peaks including those for carvone were observed, GC/MS analysis of ether extracts of the crude enzyme reaction products verified that carveol was the principle reaction product (data not shown).

Discussion

On the basis of morphology, growth characteristics, and partial 16S ribosomal RNA gene sequence, we have tentatively identified thermophilic isolate BR425 as a new strain of *Bacillus pallidus*, with confirmation awaiting more extensive examination. *Bacillus pallidus* was first described by Scholz, et al (15) as a dominant member of yeast factory sewage and in

Table A4 Stimulation of *B. pallidus* BR425 pinene hydroxylase activity by electron acceptors

Additions	Enzyme activity (U/ml)
0	0
0.1 mM FAD	0.04
1 mM FAD	0.47
1 mM FAD and 0.25 mM ferricyanide	0.60
1 mM FAD and 0.5 mM ferricyanide	0.94
1 mM FAD and 1 mM ferricyanide	2.1
1 mM FAD and 1 mM ferricyanide*	2.3

* anoxic conditions by nitrogen flushing

municipal sludge, and a recent isolate has been found to degrade both aromatic and aliphatic nitriles (6). In contrast to a previously isolated thermophile *B. stearothermophilus* BR388 which could degrade limonene but not pinene (4), isolate BR425 demonstrated a fairly broad monoterpene substrate range, but with limited growth due to limited monoterpene solubility and monoterpene toxicity.

In this and other studies of monoterpene degradation (16, 18), large numbers of metabolites have made monoterpene pathway determinations difficult. In BR425, the presence of both oxidized bicyclic and monocylic intermediates suggests either the existence of separate pathways for these intermediates, mechanisms for interconversion of these structural isomers, or oxidation steps with broad specificity. While cloning of the pathway genes and examination of participating enzymes will be required and are underway to resolve this question, our working hypothesis is that carveol and carvone are central intermediates in a common branched pathway shown in Figure A3. This hypothesis is based on the ability of BR425 to grow on carvone and carveol, production of these intermediates during growth on both limonene and pinenes, and the common but as yet unidentified intermediate found during growth on either pinene or carvone. Since growth was not

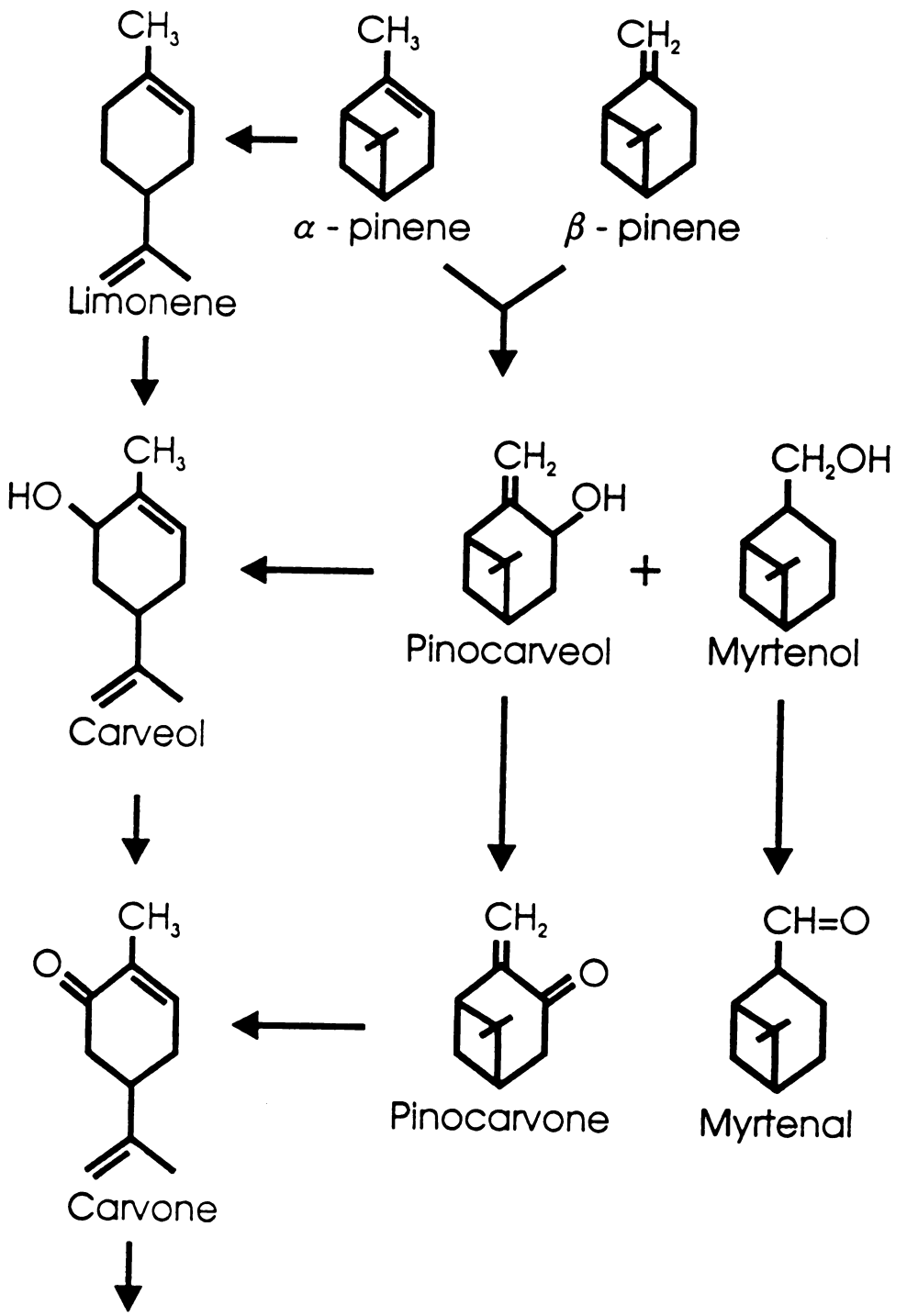

Figure A3 Hypothetical pinene degradation pathway for *Bacillus pallidus* BR425

observed on pinene oxide, no pinene oxide was observed in pinene metabolite examinations, and no pinene oxide lyase activity was observed in BR425 cell extracts (data not shown), we conclude that formation of carveol from pinene oxide by BR425 is unlikely.

The pinene hydroxylase activity observed in initial experiments with BR425 crude extracts differs from that expected for a monooxygenase, in that electron acceptors rather than electron donors serve as cofactors, and because enzyme inhibition was observed under anoxic conditions. Although detailed studies including $H_2{}^{18}O$ incorporation are required to characterize this hydroxylase activity, these initial results suggest that the pinene hydroxylase may resemble p-cresol hydroxylase (9) and nictotinamide hydroxylase (10), which hydroxylate by hydrolysis of an oxidized intermediate rather than by introduction of molecular oxygen. It will be of interest to determine the extent of similarity of this enzyme with the limonene hydroxylase of *B. stearothermophilus* BR388, which catabolizes limonene through a perillic acid pathway.

Acknowledgments

We gratefully acknowledge support for this research by the MSU Center for Plant Lipids and Starches, State of Michigan Research Excellence Fund. Mass spectral data were obtained at the MSU-NIH Mass Spectrometry Facility supported in part by a grant (RR00480) from NIH National Center for Research Resources.

References

1. Andews, R.E., L.W. Parks, and K.D. Spence. 1980. Some effects of Douglas fir terpenes on certain microorganisms. Appl. Environ. Microbiol. 40: 301-304.

2. Best, D.J., N.C. Floyd, A. Magalhaes, A. Burfield, and P.M. Rhodes. 1987. Initial steps in the degradation of alpha-pinene by *Pseudomomas fluorescens* NCIMB 11671. Biocatalysis 1: 147-159.

3. Chang, H.C., and P. Oriel. 1994. Bioproduction of perillyl alcohol and trlated monoterpenes by isolates of *Bacillus stearothermophilus*. J. Food Sci. 3: 660-662.

4. Chang, H.C., J. Gage, and P. Oriel. 1995. Cloning and expression of a limonene degradation pathway from *Bacillus stearothermophilus* in *Escherichia coli.* J. Food Sci. 60: 551-553.

5. Colcousi, A., K. M. Saquib, and D.J. Leak. 1996. Mutants of *Pseudomonas fluorescens* NCIMB 11671 defective in the catabolism of α-pinene. Appl. Microbiol. Biotechnol. 45: 822-830.

6. Cramp, R., M. Gilmour, and D.A. Coman. 1977. Novel thermophilic bacteria producing nitrile-degrading enzymes. Microbiology 143: 2313-2320.

7. Gibbon, G.H., and S.J. Pirt. 1971. Degradation of α-pinene by *Pseudomonas* PX1. FEBS Lett. 18: 103-105.

8. Griffiths, E.T., S.M. Bociek, P.C. Harries, R. Jeffcoat, D.J. Sissons, and P. W. Trudgill. 1987. Bacterial metabolism of α-pinene: pathway from α-pinene oxide to acyclic intermediates in *Nocardia* sp. Strain P18.3. J. Bacteriol. 169: 4972-4979.

9. Hopper, D.J., and D.G. Taylor. 1977. The purification and properties of p-cresol (acceptor) oxidoreductase (hydroxylating), a flavocytochrome from *Pseudomonas putida.* Biochem. J. 167: 155-162.

10. Jones, M.V., and D.E.. Hughes. 1972. The oxidation of nicotinic acid by *Pseudomonas* Chester. Biochem. J. 129: 755-761.

11. Lindskag, A., and A. Potter. Terpene emission and ozone stress. Chemosphere. 30: 1171-1181.

12. Maltseva, O., C. McGowan, R. Fulthorpe, and P. Oriel. 1006. Degradation of 2,4-dichlorophenoxyacetic acid by an alkaliphilic haliphile. Microbiology. 142: 1115-1122.

13. Maniatis, T., E.F.. Fritsch, and F. Sambrook. 1982. Molecular cloning. Cold Spring harbor Laboratory, New York.

14. Savithiry, N., T.K. Cheong, and P. Oriel. 1997. Production of α-terpineol from *Escherichia coli* cells expressing thermostable limonene hydratase. Applied Biochemistry and Biotechnology (in press).

15. Schholz, T., W. Demharter, R. Hensel, and O. Kandler. 1987. *Bacillus pallidus* ssp. nov., a new thermophilic species from sewage. System. Appl. Microbiol. 9: 91-96.

16. Shukla, O.P., and P.K. Bhattacharyya. 1968. Microbial transformations of terpenes: part XI-pathways of degradation of α- and β-pinenes in a soil Pseudomonad (PL-strain). Ind. J. Biochem. 5: 92-99.

17. Stromvall, A.M., and G. Petersson. 1993. Photooxidant-forming monoterpenes in air plumes from Kaft pulp industries. Environ. Pollution. 79: 219-2

18. Trudgill, P.W. 1990. Microbial metabolism of terpenes-recent developments. Biodegradation. 1: 93-1005.

19. Tudroszen, N.J., D.P. Kelly, and N.F. Millis. 1977. α-pinene metabolism by *Pseudomonas putida.* Biochem. J. 168: 315-318.